Summer 2002

A microfabricated microconcentrator for sensors and chromatography

Minhee Kim
New Jersey Institute of Technology

ABSTRACT

A MICROFABRICATED MICROCONCENTRATOR FOR SENSORS AND CHROMATOGRAPHY

by
Minhee Kim

The detection and quantitative measurement of trace components is a challenging task. The key component in such an instrument is the concentration step where the analytes are accumulated before the analysis. In this research, simple and inexpensive processes for the microfabrication of microconcentrator that can be used with sensors and as an injector in GC were developed. Analytes are selectively concentrated in the microconcentrator. Rapid electrical heating of the microconcentrator releases the adsorbed species as a "concentration pulse", which serves as an injection for the detection system. The relatively small size of the microconcentrator allows it to be heated and cooled rapidly. The microconcentrator serves the dual purposes of sample concentration and injection.

The devices were fabricated on 6-inch silicon substrate using standard photolithographic processes. First, a microheater embedded in silicon wafer was fabricated. The channels were lined with a conductive layer by sputtering metal film through which an electric current could be passed causing Ohmic heating. The preconcentration was done on thin-film polymeric layer deposited in the channel. Rapid heating of the conductive layer caused the "desorption pulse" to be injected into the sensor/detector. Several channel configurations were fabricated with a width between 50 to 456 μm, depth between 35 and 350 μm and length between 6 and 19 cm. The separation distance between the channels was varied such that the entire microheater

fitted in a $1cm^2$ area. Due to their small size, the microconcentrators could be fabricated more than 50 at a time on a 6-inch silicon wafer.

In the first part of this research, the heating characteristics of the microheaters are studied. Deposition of metals to form a resistive heating element in microchannels was demonstrated. It was found that temperature as high as 360°C could be attained in a ten seconds. The microconcentrator was effective as a concentrator plus injector. It exhibited high signal enhancement and precision.

A MICROFABRICATED MICROCONCENTRATOR FOR SENSORS AND CHROMATOGRAPHY

by
Minhee Kim

A Dissertation
Submitted to the Faculty of
New Jersey Institute of Technology and
Rutgers, The State University of New Jersey – Newark
Doctor of Philosophy in Chemistry

Department of Chemistry and Environmental Science

August 2002

APPROVAL PAGE

A MICROFABRICATED MICROCONCENTRATOR FOR THE SENSORS AND CHROMATOGRAPHY

Minhee Kim

Dr. Somenath Mitra, Dissertation Advisor — Date
Professor of Chemistry and Environmental Science, NJIT

Dr. Kenneth Farmer, Committee Member — Date
Associate Professor of Physics, NJIT

Dr. Dencho Ivanov, Committee Member — Date
Director of Microelectronics Research Center, NJIT

Dr. Barbara Kebbekus, Committee Member — Date
Professor of Chemistry and Environmental Science, NJIT

Dr. Durgamadhab Misra, Committee Member — Date
Associate Professor of Electrical and Computer Engineering, NJIT

Dr. Nicholas Snow, Committee Member — Date
Associate Professor of Chemistry, Seton Hall University

BIOGRAPHICAL SKETCH

Author: Minhee Kim

Degree: Doctor of Philosophy

Date: August 2002

Undergraduate and Graduate Education:

- Doctor of Philosophy in Environmental Science,
  New Jersey Institute of Technology, Newark, NJ, 2002

- Master of Science in Applied Chemistry,
  New Jersey Institute of Technology, Newark, NJ, 1998

- Bachelor of Science in Chemical Engineering,
  Rutgers University, College of Engineering, New Brunswick, NJ 1995

Major: Environmental Science

Presentations and Publications:

M. Kim, S. Kishore, D. Misra, and S. Mitra,
"Micro-machined heater for microfluidic devices",
submitted to Sensors and Actuators.

M. Kim and S. Mitra,
"A Microfabricated Microconcentrator for Sensors and Chromatographic Applications",
submitted to Analytical Chemistry.

M. Kim and S. Mitra,
"A Microfabricated Microconcentrator for Sensors and Gas Chromatography"
will be presented in μTAS, Nara, Japan, November 2002.

M. Kim and S. Mitra,
"A Microfabricated Microconcentrator for Sensors and Chromatography",
presented in 25th International Symposium on Capillary Chromatography,
Palazzo Dei Congressi, Riva Del Garda, Italy, May 2002.

BIOGRAPHICAL SKETCH
(Continued)

M. Kim and S. Mitra,
"Design and Characteristics of Microconcentrator",
presented in 223rd American Chemical Society National Meeting, Orlando, Florida, April 2002.

M. Kim, S. Kishore, D. Misra, and S. Mitra,
"Micro-concentrator interface for real-time VOC sensors",
presented in Electro Chemical Society 200th Joint Meeting, , San Francisco, CA, September 2001.

M. Kim, S. Kishore, S. Mitra and D. Misra,
"Microfabricated Heater for Microfluidic devices and other applications",
Korean Scientist and Engineers in America – North Region Conference, Fort Lee, NJ, April 2001.

M. Kim, S. Kishore, D. Misra, and S. Mitra,
"Design, Fabrication, and Characteristics of MEMS heater",
presented in Electro Chemical Society 106th Meeting, , Toronto, Canada, September1999

This dissertation is dedicated

To my God the Father, Maker of Heaven and Earth, who is My Savior and the source of my life. He ordered my steps in every aspect of this study, and, as with all of my life, I recognize my utter reliance on Him. I thank God for the marvelous ways He has brought people into my life that have helped me achieve my goal. Thank God for making the impossible possible, for moving barriers with His everlasting love and for shining His light of hope in the dark world of academia.

To my mom and dad who have helped me grow in faith in the Lord. Their many sacrifices and understanding have made this scholarly journey a successful one. Thank you for believing in me even when I didn't believe in myself. I am very grateful for your endless love, unselfishness and constant prayers.

To my sister, Dr. Minah Kim, and my brother-in-law, Sanghyok Yon who have been tremendous source of support and encouragement. Their living example of hard work and perseverance has been motivations in my life and my work. Thank you for your prayers and guidance.

To my brother, Ernie Y. Kim, who is always supportive. Thank you for the words of encouragement and patience. Your sense of humor has been a great help in overcoming many of the difficulties, which arose throughout my doctoral program.

Without God and my precious family, I could never have achieved the many accomplishments that I have attained in my academic and professional career. In all areas of my life I trust them, and this research was no exception.

ACKNOWLEDGMENT

The pursuit of this dissertation has been one of the biggest undertakings I have attempted in my life. With all that I have expended in this exercise, I recognize that I could not have achieved what I have without the support of many people.

I acknowledge, first and foremost, my God to Him be the glory for being my rock and my foundation. Thank Him for allowing me to know and experience that I can do all things through Jesus Christ who strengthens me.

I would like to express my deepest appreciation to my dissertation advisor, Dr. Somenath Mitra, who has played an important role in my scholarly development, and I owe him an immense debt of gratitude. I am very thankful that he has supported and advised me throughout my academic career and writing this dissertation. He was a source of encouragement. I am grateful for his assistance and patience to bring this dissertation to completion.

I have been blessed by the personal commitment of my dissertation committee to helping me achieve this academic accomplishment. I would like to acknowledge Dr. Kenneth Farmer, Dr. Dencho Ivanov, Dr. Barbara Kebbekus, Dr. Nicholas Snow and Dr. Durgamadhab Misra for their many constructive suggestions and constant support.

I also acknowledge Dr. Rajendra Jarwal, Dr. Suresh Sampath and Mr. Kenneth O'Brien for teaching me the detail procedures in Cleanroom step by step. I am thankful NJIT Cleanroom staff for proving a warm and friendly working environment.

Special thanks to New Jersey Commission on Science and Technology through the New Jersey MEMS Initiative and USEPA Center for Airborne Organics for the financial support.

I want to thank my very dear friend, Anthony San Juan for his friendship and encouragement that kept me focused and challenged. It would be a long list to mention all the other friends I am indebted to. I gratefully thank all of them. Thanks to all my colleagues, friends, faculty, administrators, staff who participated in my study and kept me to my self-imposed timelines.

I save the last acknowledgement for my wonderful family who have supported me through many years of school, many achievements, as well as disappointments- I share this accomplishment joyfully and gratefully with you.

May God reward all of them with hundreds of what they have provided me.

TABLE OF CONTENTS

TABLE OF CONCENTS
(Continued)

LIST OF FIGURES

LIST OF FIGURES CONTINUED
(Continued)

LIST OF TABLES

Figure **Page**

CHAPTER 1

INTRODUCTION

1.1 Miniaturization of Chemical Analysis Systems

Miniaturization is a growing trend in the field of analytical chemistry [1,2]. Over the past decade the development of microfabricated systems for analytical techniques has become a dominant player in the physical and biological sciences [3-5]. Influenced by the success of the microelectronics industry, chemists and biologists, together with physicists and engineers, are striving to miniaturize conventional laboratory devices and procedures down to the size of matchboxes [6,7]. Also, interest in miniaturized analytical systems has been stimulated by the fact that physical processes can be controlled more precisely when instrumental dimensions are reduced to the micro size. It has primarily been driven by a need to perform analytical measurements on small sample volumes so that rapid, on-line measurements at low concentrations are possible. Major applications are in fields such as DNA analysis, drug discovery, pharmaceutical screening, medical diagnostics and environmental analysis.

The success of miniaturized systems depends on the development of integrated devices (also known as micro total analysis systems, μ-TAS). These incorporate all necessary elements to perform a chemical analysis, on a single chip, and preferably can do without the need for a conventional laboratory [8,9].

μ-TAS is designed to carry out full-scale analyses from sample introduction, separation and detection, on a single, miniaturized device [10-14]. Figure 1.1 shows the typical protocol for μ-TAS that can be used for chemical analysis [15-17]. It shows that

four stages in measurement that include collection, preparation, processing and analysis. Each stage of a conventional method needs to be replaced (at least partially) with a miniaturized device. The miniaturized detectors in general do not possess the same analytical power as their bench-top counterparts. The integration in μ-TAS is important to enhance selectivity and sensitivity of the miniaturized device to a level comparable to its lab-scale counter part.

System integration also has one of the most significant roles in miniaturization. The quest for miniaturization will lead to better process intensification, since a μ-TAS would benefit from the fact that it could consist of several system elements, and each optimized for its own specific function. Miniaturization, in conjunction with integration of multiple functionalities can enable the construction of structures that exceed the performance of traditional macroscopic systems, can provide an abundance of new functionalities and offer the potential of low-cost mass production.

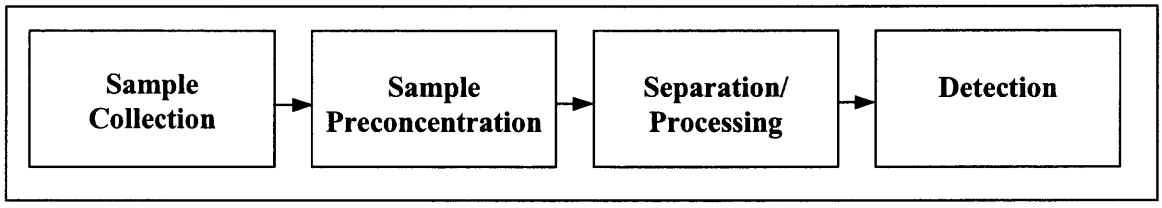

Figure 1.1 Typical protocol used for μ-TAS for analytical science.

The advantages associated with μ-TAS include:

- Increased speed and higher sample throughput
- Reduced reagent consumption both in energy and chemicals and waste generation both heat and chemicals
- Reduced manufacturing and operating costs per analysis

- Improved efficiency with respect to sample size, application, response times, experimental throughput and automation.
- The possibility of parallel processing.

1.2 Microfabricated Instrumentations for Environmental Monitoring

The determination of the trace levels of organic pollutants in aqueous/gaseous samples are of important because from a public health and regulatory perspective. For example, airborne aromatic compounds such as benzene, toluene and xylene are toxic even at ppb concentrations and lead to tropospospheric ozone formation. Highly sensitive analytical techniques are needed for their detection in the field that can be used in this type of analysis. Development of several on-chip analytical instruments has been reported. The details are described on following section. A micro-fluidic device by using flame ionization detector as the detection method, which enables to identify and quantify atmospheric levels of VOCs, was reported. Microchip-based separation techniques, as an essential element in the development of fully integrated micro-total analysis systems, were integrated with several detectors for environmental analysis. Microfabricated analytical instrumentations are envisioned to become powerful tools for environmental monitoring.

1.2.1 Miniaturized Gas Chromatography

Gas chromatography (GC) is one of the most reliable analytical tools commonly employed in the laboratory setting for environmental measurement. The components of a mixture can be separated, identified, and their concentrations quantified using a GC. In their most common configuration, they tend to be large, fragile and expensive table-top

instrumentation. In consonance with the Environmental Protection Agency (EPA) and National Institute of Occupational Safety and Health (NIOSH) federal mandates for accomplishing on-site chemical analyzes, several investigators have focused their attention toward realizing portable and robust GC systems. Development of a miniaturized gas chromatographic system was reported as early as in 1979 [18-25]. In fact, it was the first microchip-based analytical system fabricated on silicon. This device included an injection valve and a 1.5 m long separation column all fabricated on a single silicon wafer. A thermal conductivity detector was fabricated on a separate wafer and mechanically clamped to the wafer containing the column. Although this gas chromatograph was able to separate simple mixtures in a matter of seconds, the response was lukewarm due to the difficulties in producing homogeneous stationary phases and adequate phase ratios that led to unsatisfactory performance.

Development of a new miniaturized gas chromatography (referred as micro GC) system was reported [26-31]. This miniature GC system consists of five components: a miniature sample injector that incorporates a 10 μl sample loop; a 0.9 m long, rectangular-shaped (300 μm width and 10 μm height) capillary column coated with a 0.2 μm thick copper phthalocyanine (CuPc) stationary phase; and a dual-detector scheme based upon a CuPc-coated chemiresistor and a commercially available, 125-μm diameter thermal conductivity detector (TCD) bead. Modern silicon micromachining and VLSI circuit processing techniques were employed to fabricate design the interface between the sample injector and the GC system's column, the GC system's column itself and the dual-detector cavity. A novel integrated circuit thin film processing technique was developed to deposit the CuPc stationary phase, which is a nearly homogenous thin-film, coating on

the GC system's column walls micromachined in the silicon wafer substrate and the Pyrex(R) cover plate which was bonded electrostatically. In this micro GC, the separation and detection of NH3 and NO_2 in less than 30 minutes were demonstrated when it operated isothermally (55-80 °C).

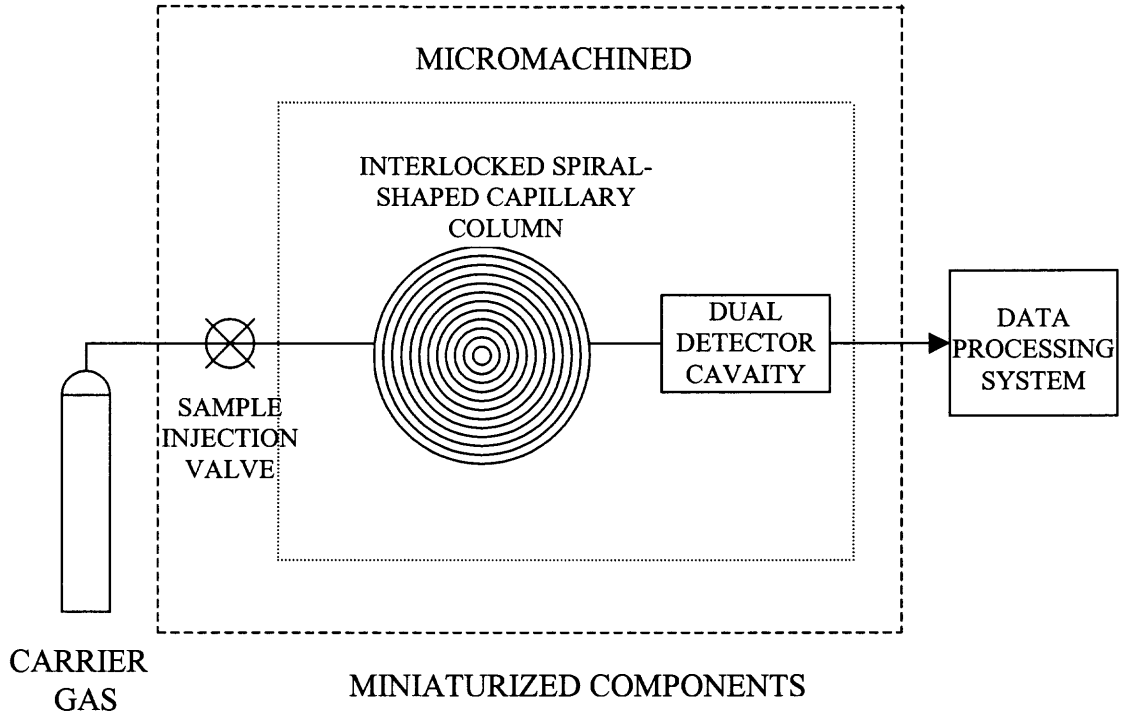

Figure 1.2 Functional block diagram of the micromachined GC system.

There are several commercially available micro GCs. The instrument from Varian, Inc. has a dimensions of 5.9 x 11.8 inch, and features one to four plug-and play GC columns, each of which has a separate pneumatics, injector, column and detector, enabling the user to generate more data 10-50 times faster than conventional GCs. A Chrompack 2002 micro-GC system, as shown in Figure 1.3, equipped with two gas chromatographic modules [32]. Each module consists of an injector, two heated columns

and a micromachined thermal conductivity detector. This micro GC consists of an injector, which is etched in a glass wafer, pneumatically actuated valves, a micro sampling loop and flow restrictors. For optimum performance these were a conventional open tubular capillary columns.

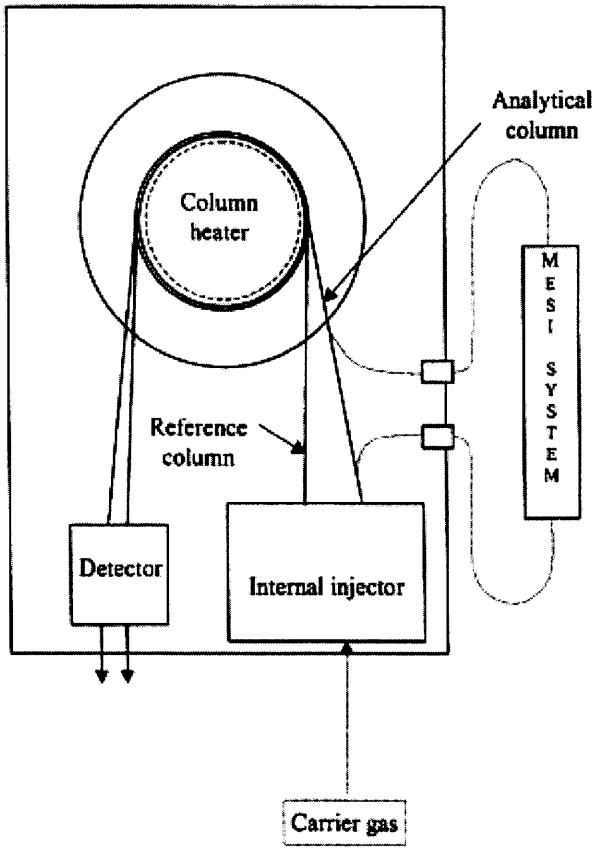

*MESI = Membrane extraction with a sorbent interface

Figure 1.3 Schematic of a micro-GC module.

The commercially available micro GCs have a rather limited scope of applications. Most of them have poor sensitivity. However, the sensitivity can be very much improved by sample preconcentration.

Development of microfabricated silicon gas chromatographic micro-channels was also reported [33]. These columns range from 1m to 1.5m in length on a $1cm^2$ silicon chip. Polymeric stationary phases impart both analyte selectivity and time discrimination.On-chip temperature ramping gives these devices excellent selectivity with a rapid response.

Advantages of micro GC are a small sample volume (x 10^{-6} cm^3) and short retention times (~ 160 s). And gas chromatograph with a cryogenic separation column has been used for the analysis of hydrogen isotope gas mixture in the fusion fuel cycle [34]. However, cryogenic GC has the disadvantage of long retention time, typically a few 10 min [35]. However, it is not suitable in applications such as process control that require faster response. It should be noted that these micro GCs may still require off-chip sample preparation such as liquid extraction, pyrolysis-derivatization and preconcentration.

1.2.2 Chip - Mass Spectrometry

Mass spectrometry is another analytical tool used for environmental monitoring. Presently available mass spectrometers use relative bulky mass analyzers. Large dimensions of several tens of centimeters require low pressure of 10^{-4} mbar or less, which requires a two-stage pumping system. Thus the pumping system accounts for a considerable share of the overall size and cost. The above mentioned disadvantages can be greatly reduced by using a mass spectrometer fabricated as a micro-system. The small

separator length of 1.5 mm facilitates mass separation at a 1-10 Pa pressure, hence requiring simpler vacuum systems.

Several microfabricated devices have been reported for coupling capillary electrophoresis to mass spectrometer [36-37]. For example, microelectric impedance spectroscopy has been developed for the electrophysiological characterization of cells. They were applied to the analysis of proteolytic digests as well as peptides. Two mass spectrometer analyzers, a triple quadrupole and time of flight, were connected separately to microfluidic devices through nanoelectrospray emitters to perform trace analysis of membrane proteins and carnitines in human urine. A device that integrated the synthesis of compound and a detection mode that relied on time-of-flight mass spectrometry was presented. This system also allowed the parallel processing, in real time, of multicomponent reaction subreactions.

A modular microsystem including an autosampler, microfluidic separation device, and interface for nanaoelectrospray mass spectrometry was presented. Such a system was able to perform sequential injections and separations of up to 30 samples/hour.

A chip-based CE/MS system has been reported to make quantitative determinations of drugs in human plasma. A 15-amol-sample detection limit by coupling a chip and a mass spectrometer has been achieved.

An advantage of miniaturization is generation of high field strength at low voltage exploited. Even high field strength due to the small dimensions of a micro-system can greatly enhance portability. Due to the small size, low power and low gas consumption the micro mass spectrometer is suited for self-sufficient mobile analysis system in application such as pollution and process monitoring. However, present day micro mass

spectrometers do not have the figures of merit of the macroscopic mass spectrometers and their detection limits are high, which ranges in the order of several hundred of ppm.

1.2.3 Microfabricated Sensors

Microfabricated devices require new approaches to sensor technology to exploit the full potential of microsystem integration, and to provide a complete solution for complex and tedious analytical problems. Development of several sensors has been reported [38-42]. SAW sensors are well known their high sensitivity for chemical and gas sensing. A SAW device is characterized in that a surface acoustic wave is electrically excited in a piezoelectric plate substrate by use of a metallic interdigital transducer (IDT) structure. When a SAW device is coated with organic and /or inorganic materials, it acts as a chemical sensor while the specific environmental analytes are adsorbed to its surface. Figure 1.4 shows a schematic of SAW sensor. As shown in Figure 1.4, SAW devices consist of a piezoelectric substrate, typically quartz, and two interdigitated transducers formed by photolithographic patterning of a thin metal layer.

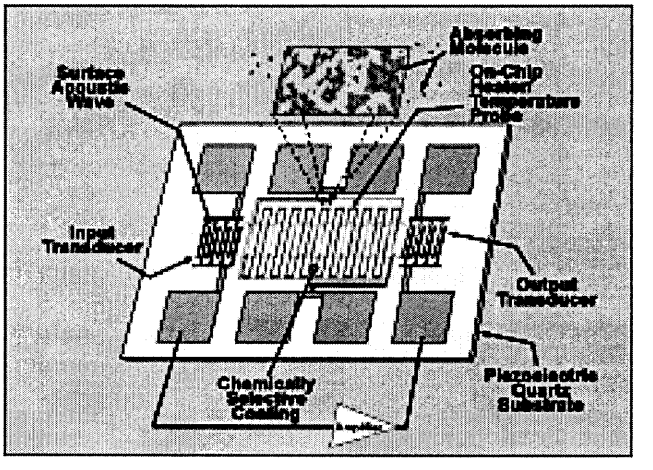

Figure 1.4 Schematic of a surface acoustic wave (SAW) sensor.

Development of mass-sensitive sensor arrays with polymer-coated SAW device has been reported [43-45]. Especially, SAW resonator based sensors are accepted to have the best sensing properties for organic gas detection [46]. A SAW sensor array based on eight non-continuously working oscillators equipped with differently coated SAW sensors as shown in Figure 1.5. The sensor array approach provides greatly increased selectivity and reliability in field environments over a single sensor. Single sensors do not have high selectivity to discriminate against interfering species. In addition, sensor arrays offer the possibility of detecting and quantifying multiple analytes with the same system. The compact SAW sensor array systems envisioned would convert data into chemical information and communicate it in a form necessary for decision-making.

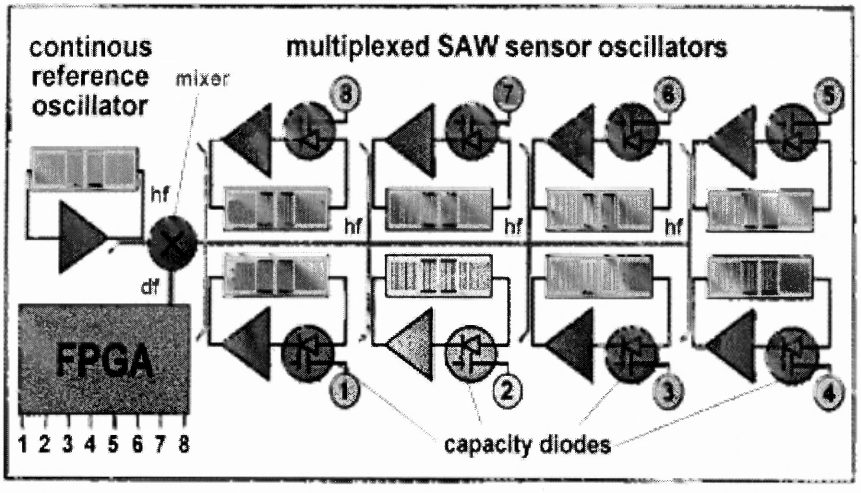

Figure 1.5 Schematic setup of the sensor array, consisting of eight multiplexed SAW oscillators with capacity diodes.

A variety of portable SAW sensor array systems have been developed. They have been designed, built and field tested to provide rapid, reversible, sensitive, and quantitative detection of individual volatile organic compounds. The sensor responses and chemical concentrations were observed for trichlorethylene using the portable SAW sensor as shown in Figure 1.6.

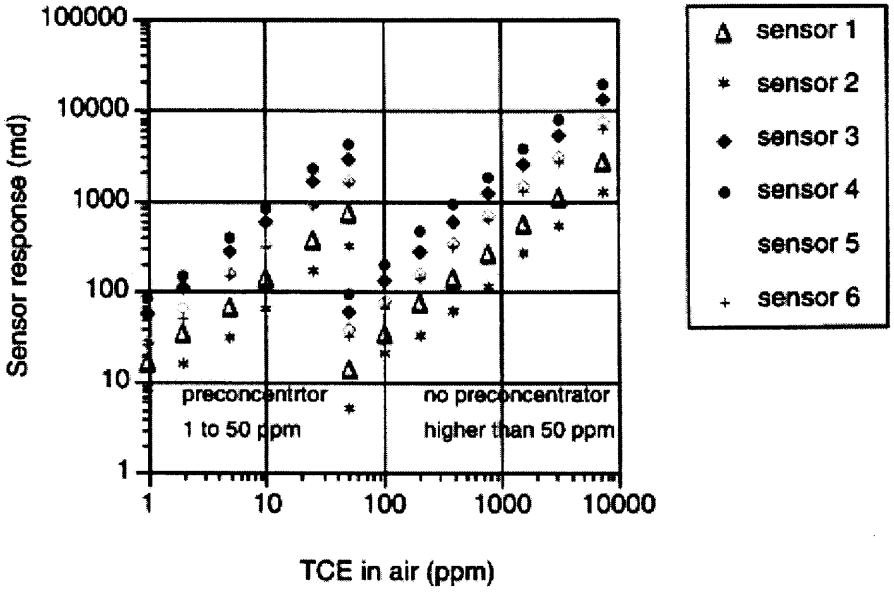

Figure 1.6 Linear sensor responses to trichloroethylene from 1 to 10,000 ppm.

The latest and smallest system is housed in a 5.5"x3.3"x1.5" plastic case and includes batteries for portable or field operation developed by Sandia National Laboratories as shown in Figure 1.7 [15]. However, this system consists of only a single SAW sensor. It is still under way to design and built a portable instrument based on a

SAW sensor array using selective coating on separate sensors to provide simultaneous chemical identification and quantitation of multiple VOCs.

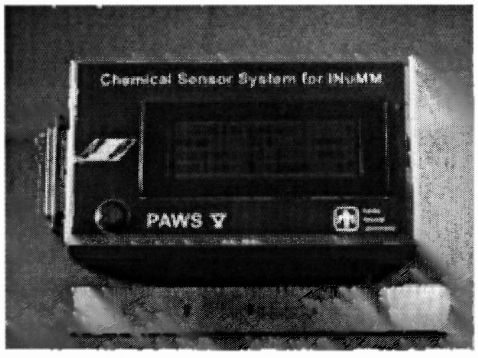

Figure 1.7 Picture of battery operated portable SAW sensor.

SAW sensor technology will become the basis for practical, fieldable solutions to characterization and monitoring problems. However, it is still under way to design and build a portable instrument based on a SAW sensor array using selective coatings on separate sensors to provide simultaneous chemical identification and quantitation of one or more VOCs.

The advantages of the SAW vapor sensor technology include

- Rugged planar design of the devices
- Suitability of polymer-coated devices for use in arrays with pattern recognition
- Fast response times (seconds)
- Rapidly reversible responses (the selective material is not altered by the vapor)
- Flexibility of the array approach to be adapted to many detection problems

Development of a tin oxide sensor has been reported. SnO_2 films are commonly used as gas sensors due to their high sensitivity and selectivity towards various toxic

gases in urban environments. These sensors also present short response times to gases, as well as good reproducibility and repeatability. The gas detection capability of these sensors is based on the variations of the sensor resistance caused by the adsorption of gas on the sensor surface. Also, a sensor array of tin oxide sensors has been reported. Using a sensor array of 15 thin film tin oxide sensors, the classification of six VOCs single gases and the multicomponent analysis of VOCs gas mixtures were possible. Unlike most semiconductor sensors, tin oxide based sensors showed excellent linear characteristics. However, there was inadequate long-term stability, which is of considerable significance for the practical use. For example, the case for use of this type of sensors in warning devices both in private household and industrial applications, for which is not possible to schedule recalibaration since the cost of such recalibaration would be relatively high. One of the reasons for inadequate long-term stability is the change of matalization. At high temperature, a metal film could create volatile oxides, which might destroy the sensor heater. This decreases the effective heating of the sensor and thus reduces the sensor temperature. As a result, the sensor resistance is usually increased and the gas sensitivity is altered.

The miniaturization of chemical sensors made possible by silicon processing leads to opportunities for mass production of inexpensive sensors with low power consumption, fast response, and increased sensitivity to small amounts of chemical species. However, most of them suffer from problems associated with lifetime, stability and chemical interference. In fact, to perform a satisfactory chemical analysis in the laboratory a complete system involving several steps in usually used. A sensor faces significant challenges in approaching the detection limits and selectivity of many

laboratory procedures. The increasing needs in monitoring and detection of various chemicals and gases has added new impetus to the research and development of low cost sensors. In principle, sensors can provide real-time (or near real-time), on-line measurements. Furthermore, it is desirable that the sensors be completely automated, and not requires additional chemical reagents or sample preconditioning. Figures of merits are necessary for all measurements such as high sensitivity, selectivity, reproducibility, short response time and long-term stability. To solve real-world problems, the sensors need to meet these requirements. However, most gas sensors do not have the figures of merit that are need in many monitoring applications. They may suffer from problems such as non-linearity, low selectivity and sensitivity. In trace measurements applications such as in environmental monitoring and chemical vapors detections, the biggest draw back has been the low sensitivity and high detection limit of the sensors.

1.3 Preconcentration on Chips

Detection sensitivity is one of the few performance parameters of an instrument for chemical analysis that does not directly benefit from system miniaturization. This is because the dimension of the analysis system is minimized, the available detection volume is reduced. For example, when performing capillary electrophoresis on microfabricated chip device, injection volumes may typically range between 10^{-14} – 10^{-10} dm^3 [47]. This implies that for a diagnostically relevant sample concentration of 1 nm, only 10 – 1000 molecules are available for analysis. Since the number of molecules actually available for detection decreases drastically as detector volumes are reduced in size, this will result in high detection limit. If the injection volume is reduced much

further a point is soon reached at which no analyte molecules at all will be introduced into the analysis system. Moreover, even for analyte volumes on a pL scale, it is evident that detection becomes a key issue in determining the practicality of microfluidic systems. And this is also true for the miniaturized gas chromatography, as the column dimensions are further reduced, so is the available detection volume. Hence, many detection principles are concentration-dependent and surely a final frontier is reached when there is only one molecule left in the detection volume.

Many approaches have been undertaken to overcome the limitation described on the above. Development of the methods for on-chip detection is the one way. It is clear that high-sensitivity detection is essential when performing any kind of analysis on a small scale. Many literatures demonstrate that the methods for on-chip detection include laser-induced fluorescence (LIF), chemiluminescence, electrochemistry, refractive index variation, Raman spectroscopy and electrochemiluminescence methods [49,50]. Of these, LIF continues to be the most applied form of optical detection in conjunction with microfluidic chips, due to its exceptional sensitivity and low mass detection limits. Most of small volume detection within planar chip devices has conventionally been based around optical measurements. This is primarily due to the optical properties of the materials used in chip fabrication. For example, the most common substrates include glass, quartz and polymeric materials, all of which possess good transparency in the visible regions of the electromagnetic spectrum. However, LIF techniques suffer from significant drawbacks that prohibit their use universally. These include LIF detection requires a large, expensive off-chip supporting optical system that greatly compromises the benefits of miniaturization and portability, and the fact that the majority of molecular

species do not fluoresce or are not easily converted to fluorescent species. Also, most microfluidic chip devices have been developed for specific application such as DNA/RNA separations, small-molecule organic synthesis, DNA amplification, immunoassays and cell manipulation [50]. In many of the above applications a single analyte is targeted for analysis. However, more usually structural identification and quantitation of individual sample components is highly desirable or even necessary. On-chip spectroscopic detection cannot easily provide this information and consequently alternative analytical techniques must be considered. Therefore, the development of new detection protocols in therefore of considerable importance.

As an alternative to these studies, the research might be approached from the other side that is to increase the number of available sample molecules in the detection volume prior to their detection by proving some kind of preconcentration step. Aiming to overcome the above-mentioned drawbacks by the on-line generation of a flow of a homogeneously enriched gaseous sample is the preconcentration method based on the principles of equilibrium absorption.

Sample preconcentration is necessary where trace analysis of organics is desired, and the detection sensitivity is too low to reliably detect and quantify the analysis. In our previous studies, we have reported the use of microtrap. The microtrap interface had been explored for directly introducing air sample into a mass spectrometer (MTMS). Compared with other methods, microtrap offers the convenience of being both a sample concentrator and injection device. By trapping organics on a sorbent material to increase the sample amount for detection, the detection limits can be reduced to ppt level. Sampling time varies from under one minute to several minutes depending on the

detection level required by the application. Unlike the other methods, the thermal desorption of the microtrap produces a concentration pulse into ionization chamber, which generates a peak instead of a platform as detection signal. By using a microtrap, we have reported the improvement of signal to noise rations at very small concentrations.

A common technical challenge for many trace analyte detection applications concerns the ability of a detector to collect the sample efficiently, both to achieve a certain limit of detection and to achieve that sensitivity within a reasonable time frame. Detection sensitivity for many analytes can be significantly improved by using some type of preconcentration step.

However, preconcentration devices based on conventional adsorption-thermal desorption techniques cannot be directly coupled to micro GC without strict miniaturization. These demands impose great difficulties in the construction of portable analytical instrumentation based on high-speed narrow-bore GC techniques. Microchip-based preconcentration techniques are essential elements in the development of fully integrated micro-total analysis systems, which are envisioned to become powerful instruments for obtaining and assessing analytical data in research, industry, and everyday life.

CHAPTER 2

RESEARCH OBJECTIVE

The key component in trace analysis is the concentration step where the analytes are accumulated before the analysis. The objective of this research is to micromachine a concentrator (referred to as the microconcentrator) on a silicon substrate that can be integrated with a sensor/detector to enhance the sensitivity. Another application demonstrated here is a concentrator cum injector for a micro gas chromatography. The microconcentrator is a miniaturized sorbent trap fabricated on a microchip so that a sensor or detector can be integrated on the same chip.

The microconcentrators were fabricated on six-inch silicon substrate using standard photolithographic processes. The fabrication steps are discussed in detail. The microconcentrator is composed of microchannels etched in silicon. The channels were lined with a resistive layer through which an electric current could be passed causing Ohmic heating. The fabrication and testing of the metal deposited heaters are studied. The preconcentration was done on thin-film polymeric layer deposited above the heater in the channel. Rapid heating of the resistive layer caused the "desorption pulse" to be injected into the sensor or a detector. Due to their small size, the microconcentrators could be fabricated more than 50 at a time on a 6-inch silicon wafer.

In summary the objectives of this research were:

- Development of microheater on a chip
- Study the heating characteristics of microheater
- Fabrication of the microconcentrator on a chip
- Integration of the microconcentrator with FID detector
- Study the characteristics of microconcentrator

CHAPTER 3

A MICROMACHINED HEATER

3.1 Introduction

Microfluidic devices are being used in various applications, such as, chemical analysis, drug discovery, electronics chip cooling, flow sensors and bio-medical devices [51]. There has been a growing interest in microfluidics for use in various analytical applications such as gas chromatography [52-54], liquid chromatography [55], and capillary electrophoresis [56-58]. It has been demonstrated that it is possible to put a conventional chemical laboratory onto a single microchip to produce a large numbers of chemical micro analytical systems [59]. These micro-electro-mechanical systems (MEMS) have improved the performance by fast analysis and offer functional and economic benefits. Performance enhancement, high throughput, lower power consumption, the reduction of the sample size, and low cost are some of the advantages of these devices. Moreover, the combination of chemical analysis and traditional electronics on a single silicon chip can lead to fast and inexpensive manufacturing processes [60]. Noteworthy among the different applications is microfabricated capillary electrophoresis used in DNA analysis.

Many microfluidic devices require technologies for temperature control because reactions and sample preparations need to be carried out at higher temperatures. It is often important to maintain a particular area of a working element heated while rest of the system is at a lower temperature [61]. The need for local microheating and maintaining a constant temperature necessitates the development and fabrication of

efficient microscaled heaters. For example, the Polymerase Chain Reaction (PCR) for DNA amplification requires fast temperature cycling which takes within 30 to 40 seconds for each cycle [62].

Development of several microfabricated heating devices has been reported [63-74]. Widely used techniques for these microheaters involve either the deposition of polysilicon layer [64,65], or the heavy doping of the silicon substrate [66,67]. Many of the current microheaters use fabrication techniques in which a selective etch of the bulk silicon followed by implant of high concentration of dopants (typical range of the ion dose is between 10^{19} to 10^{21} atoms/cm^3) to achieve a higher level of electrical conductivity of the heater region [68]. The study on micromachined heaters for thermomechanical data storage has been conducted [66]. Single-crystal silicon cantilevers with integrated resistive heaters have also been demonstrated [66]. These cantilevers were made electrically conductive by a heavy ion implant. The heater region was doped with phosphorous at 1.5 x 10^{21} atoms/cm^3 and the legs at 10^{20} atoms/cm^3 [66]. Ion implantation over a device allows the option of further anisotropical etching of the underlying substrate while providing for localized heating. However, heavy ion implantation is an expensive process [69].

Silicon On Insulator (SOI) technology is another way of fabricating microheaters and is known to be simpler than deposition of polysilicon layers, or the heavy doping of the silicon [70]. A thermally isolated microheater suspended 2μm above the wafer substrate has been fabricated using a SOI wafer with a 2 μm buried oxide layer on silicon substrate for the fabrication of heating devices [71]. This method is simpler than the other methods because it involves only one masking step. However, it also requires heavy

boron or phosphorous doping to form the conductive layer (approximately > 10^{19} atoms/cm^3). Experimental results obtained using these devices have shown that temperatures in excess of 1000 °C can be achieved with the use of very little power [71]. The heater can be as small as 500 μm^2. It has also been demonstrated that these heaters reduce contact resistance so that there is less unwanted heating at the contacts. However, once the maximum temperature is reached, any further increase in current only broadens the active area of the heating element. Thus, continued operation in this region leads to device weakening and eventually device burn out.

In this chapter, a simplified and inexpensive process for the fabrication of microheaters for microfluidic applications using standard photolithographic techniques and chemical wet etching is presented. This chapter focuses on the fabrication and testing of the metal deposited heaters. Their temperature characteristics have been studied under various conditions. The heaters were also coated with Spin-On-Glass (SOG) to see how that changed the heating characteristics. Stability of the heater under repeated pulses was also studies to simulate real-world applications. A comparison is also made with a heater of similar dimension formed by boron implantation of silicon.

3.2 Experimental

The microheaters to be used in MEMS could be fabricated on quartz or borosilicate glass wafers, two common materials for photolithographic fabrication [75]. Quartz works well in electrophoresis because it is not only a good electrical insulator, but also transparent to the UV required for absorbance and fluorescence detection. Quartz substrates also generate high electroosmotic flow rates and have favorable surface characteristics after

fabrication by etching [76]. Silicon is also popular as a microfluidic substrate because it is possible to embed both fluid-control and fluid detection by integrated circuits on one substrate. The typical fluidic devices such as microreactors and microfluidic capillaries are 2- to 3-cm^2 in size, and are made of silicon, glass, quartz, or plastic that are either etched or molded [77]. Microfluidic chambers and channels have cross-sections as low as 5 to 50μm. The etched channels and chambers are usually covered with such as Pyrex, glass or silicon to contain the sample and the reagent.

3.2.1 Fabrication

All fabrications except the ion implantation were done at the New Jersey Institute of Technology Microelectronics Research Center cleanroom. NJIT cleanroom is a 1200-sq.-ft and class 10 fabrication line. Ion implantation was carried out at Ion Implant Services (Sunnyvale, CA). Ion implantation was performed at Ion Implant Services (Sunnyvale, CA). The implantation processes were simulated using Stanford University Process Emulator (SUPREM III) simulation package.

The chip layout was done on a Sun Sparc workstation using IC tool in Mentor Graphics (Wilsonville, OR).

3.2.2 Flow Chart for Fabrication of the Microheater

The following shows a flow chart of the entire processing to fabricate the microheater. The detail traveler is shown in Appendix A.

3.2.2.1 Microheater Made by Aluminum Alloys:

Silicon Wafer

↓

Steam oxidation to grow oxide

↓

Deposition of LPCVD nitride

↓

Photolithography to pattern the nitride

↓

Reactive Ion Etching (RIE) of nitride and oxide

↓

Stripping photoresist

↓

Wet etching of the silicon

↓

Sputtering of the metal

↓

Photolithography to pattern the metal

↓

Wet etch the metal

↓

Stripping the photoresist

3.2.2.2 Microheater Made by Boron Implantation:

Silicon Wafer

↓

Steam oxidation to grow oxide

↓

Deposition of LPCVD nitride

↓

Photolithography to pattern the nitride

↓

Reactive Ion Etching (RIE) of nitride and oxide

↓

Stripping photoresist

↓

Wet etching of the silicon

↓

Patterned wafers were sent to Ion Implant Service

3.2.3 Process

A detailed description of the process is described below. The materials used for this microheater were <100> oriented, 6-inch, p-typed (boron doped), single side polished silicon wafers, with a thickness of 575 μm and a resistivity of 10-25 Ω-cm.

Each wafer was scribed on the back for identification, and then all the wafers were cleaned by using wet chemical cleaning which is usually done by rinsing in hot organic solvents followed by mechanical scrubbing. This step helped in removing the impurities and contaminants from the wafer surface. The impurities and contaminants include as airborne bacteria, grease and wax from cutting oils and from physical handling, and a variety of plasticizers which come from the containers and wrapping in which the wafers are handled and shipped. surface. Surface cleaning is important prior to high temperature processes because impurities react and diffuse at much higher rates at elevated temperatures. The most commonly used wet chemical cleaning technology is based on hot alkaline or acidic peroxide (H_2O_2) solutions. These are used to remove chemically bonded films from the wafer surface prior to critical steps. RCA cleans are based on a two-step process: standard-clean-1 (SC-1) followed by a standard-clean-2 (SC-2). SC-1 is an aqueous alkaline solution which functions to oxidize all remaining organic contaminants on the surface, while SC-2 is an acidic mixture that is effective in removing heavy metals such as cadmium, cobalt, copper, iron, mercury, nickel, and silver, alkali ions and cations. SC-1 consists of 5:1:1 volumes of DI water (H_2O) : 30% hydrogen peroxide (H_2O_2) : 20% ammonium hydroxide (NH_4OH). This solution is very effective in removing organic contaminants. SC-2 typically consists of 4:1:1 volumes of DI water (H_2O): 30% hydrogen peroxide (H_2O_2) : 37% hydrochloric acid (HCl) is effective in removing heavy metals. Each of these steps is carried out for ten minutes at 80°C under condition of rapid agitation.

The first step was steam oxidation of the wafers to grow approximately 1500 Å thick oxide layer at 950 °C for 40 minutes. The details of process conditions are:

O_2 = 75 SLM

Bubbler = 530 sccm

Temperature = 1050 °C

Time = 30 minutes

Target thickness = 3000 Å

This was followed by LPCVD to deposit the silicon nitride layer (Si_3N_4). The details of process are:

NH_3 = 120 sccm

DCS = 50 sccm

Pressure = 200 mTorr

Temperature = 775 °C

Time = 25 minutes

Target thickness = 1200 Å

The thickness measurements were done using ellipsometer. Ellipsometer is a film-thickness instruments that use a polarized laser light source. In the ellipsometer the polarized beam is directed to the oxide-covered wafer at an angle. The beam enters the transparent film and reflects off the reflective wafer surface. During its passage through the film, the angle of the beam plane is rotated. The amount of rotation of the beam is a function of the thickness and index of refraction of the film. A detector in the instrument measures the amount of rotation and an onboard computer calculates the thicknesses and refractive indices of multiple layers (such as SiO_2 followed by Si_3N_4) on a semiconductor substrate. A major advantage of this technique is that areal information can be obtained in a nondestructive manner by scanning the beam over the surface.

The next step was photolithography of 2000Å thick oxide and 1550Å thick nitride to create the patterns on the wafer surface. Photolithography is one of the most critical operations in semiconductor processing. The goal of the photolithography is twofold. First, it is to create in and on the wafer surface a pattern whose dimensions are as close to the design requirements as possible. The second goal is the correct placement called alignment. The details of the photolithography process are:

Wafer with mask film

↓

Coating with primer

↓

Coating with photoresist

↓

Softbake

↓

Cooling

↓

Mask alignment

↓

UV exposure

↓

Development

↓

Hardbake

↓

Removal of exposed photoresist

↓

Etching of mask film

↓

Removal of unexposed resist

↓

To next process

The photoresist (PR) was applied as a thin film to the substrate and subsequently exposed through a mask. The mask contains clear and opaque features that respectively prevent or allow light through define the patterns to be created in the PR layer. The areas in the PR exposed to the light are made either soluble or insoluble in a specific solvent known as developer. Here resist was retained only on the active region and was removed from elsewhere. To start with the wafer was spin primed with a pre-resist coating of a material designed to ensure good photoresist adhesion. The primer chemically ties up molecular water on the wafer surface, thereby increasing its adhesion property. The spinner dispensed the primer onto the rotating wafer; the chuck is ramped to 800 rpm for 20 sec to dry the prime layer. The wafers were then ready to be coated with photoresist. Spin coating is the most widely used technique to apply a uniform and adherent film of desired thickness. This procedure was carried out be dispensing the resist solution on the wafer surface, and then rapidly spinning the resist at 2000 rpm for 20 sec, until the resist was essentially dry.

After the wafers were coated with photoresist, they were subjected to a temperature step, called softbake. In this step, all traces of solvent from the spun- on resist are droved out, and adhesion of the resist is improved. Typically, the film thickness shrinks to about 85% of its spun-on value during this softbake step. The wafers were softbaked at 110 °C for one minute. After the wafer had been coated with resist and suitably softbaked, it was ready to be exposed to some form of radiation in order to create an image on the resist. The degree of exposure was adjusted by controlling the energy impinging on the resist. Following exposure, the resist film was made to undergo development which results in dissolution of the exposed photoresist but does not affect the unexposed regions. The wafer was then spun-dry and transported to the postake module. Following development, an inspection was performed. The purpose was to insure that the steps of the PR process up to this point have been performed correctly and to within the specified tolerance. Any inadequately processed wafers detected by this inspecting could have their resist stripped and reworked. Hardbaking was then performed at 115°C for 60 sec. The goal of hard baking is to further densify the resist so as to reduce the dissolution rate of its undissolved regions, to improve the adhesion, and to toughen the resist so that it can better withstand during reactive ion etching (RIE) etch process.

Silicon nitride and oxide were etched using Trion-Phantom. Details of process conditions are:

40 sccm CF_4

Pressure = 250 mTorr

Power = 150 Watts

Temperature = 25°C

Time = 180 sec for each cycle

RIE systems are a combination of plasma etching and ion beam etching. The combination brings the benefits of chemical plasma etching along with the benefits of directional ion milling. A major advantage of RIE systems is in the etching of silicon dioxide over silicon layers. Visual inspection was made to make sure that the nitride was etched completely. The photoresist layer that acted as an etch barrier was no longer need and was stripped subsequently.

An anisotropic etching of silicon was then performed. The wafers were immersed in the solution of potassium hydroxide (KOH 45% by volume) at 90 °C for 6 hrs at an etch rate of 1.66 μm/minute. The KOH etch is a mixture of 45% KOH in water. The solution is heated to 90 °C in a stainless steel water bath. A lid is placed over the beaker which causes condensation of the solution to be dripped back into the beaker, maintaining a constant chemical composition and therefore constant etch rate. The etch rate will depend on the doping and crystal orientation of the silicon and the type and temperature of KOH solution used, but is typically on the order of about 1.2 μm per minute. The wafers were placed vertically, so that the gaseous by-products could escape without hindering the etch. When the wafer was etched through silicon, the etch was stopped on the nitride. The KOH etch has a very high selectivity between the (100) and (111) plane of silicon. This causes the silicon wafer to be etched at 54.7° angle with respect to the surface of the (100)-oriented wafer. After KOH etch, the wafer was cleaned using DI water.

Two different approaches were taken to form the conducting layer in the microheater. The first was deposition of metal in the channel by sputtering, and the second was doping with boron via ion implantation. The metal source used in this study was aluminum alloy, which was 99% aluminum, the rest being silicon and copper. The reason of using the silicon-aluminum alloys was to prevent the silicon in the wafer from reacting with the deposited aluminum, which could cause spiking, or short circuits [78]. Approximately one micron Al-Cu-Si metal was sputter deposited. Aluminum and its alloys are primarily used as material, which interconnects the deice structures, formed in the silicon substrate. Sputtering is the term used to describe the mechanism in which atoms are dislodged from the surface of material by collision with high energy particles. The sputtering process basically consists of four steps, ions are generated and directed at a target, the ion sputter target atoms, the ejected (sputtered) atoms are transported to the substrate, these atoms condense and form a thin film. Photolithography was performed using the metal mask. Metal etch was performed using wet etch. Selective etching solutions for aluminum alloy layers are based on a mixture of H_3PO_4 and HNO_3.

A set of etched wafers was sent to ion implantation service. Ion Implantation is a process by which energetic impurity atoms can be introduced into a single-crystal substrate in order to change its electronic properties. In ion implantation, dopant atoms are ionized, formed into a beam, and swept across the wafer. The bombarding atoms enter the substrate and come to rest below the surface. The dopant used in this study was boron.

3.2.4 Cross Sections

The Figure 3.1 shows the step by step processing of the wafer and its cross sectional view after each step.

A. The Silicon wafer was p-type. 1500 Å steam oxide was grown on the wafer.

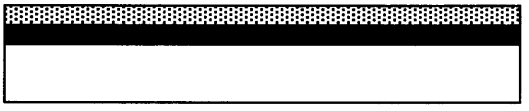

B. A 2000 Å thick silicon nitride was deposited.

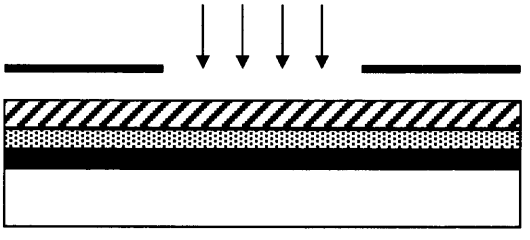

C. Photoresist was then deposited and Si_3N_4 and SiO_2 were patterned.

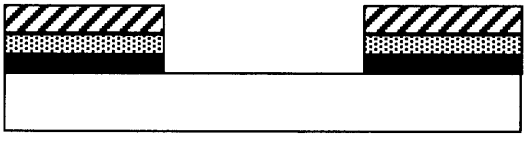

D. Si_3N_4 and SiO_2 were RIE etched.

E. Photoresist was stripped and KOH wet etch was then done.

F. Metal was sputtered.

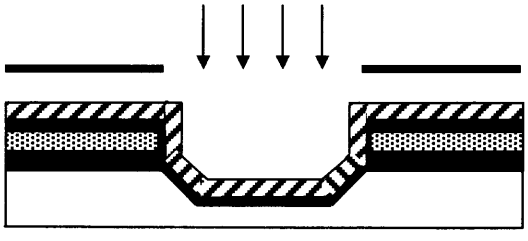

G. Photoresist was then deposited and was patterned.

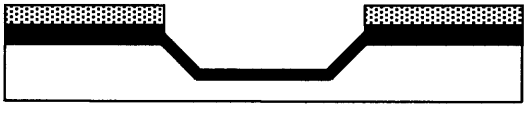

H. Metal was patterned using metal mask as shown above.

I. Spin-on-glass was coated.

Figure 3.1 Cross sectional view after each step.

3.2.5 Experimental Set-up

Once all process steps were completed, each microfabricated heater was tested individually. The heater was mounted under a four-point probe station (Cascade Microtech Inc., Beaverton, OR). Different voltages were applied to each device to test the heating characteristics as a function of time. The voltage was applied through 0.5 mm tip tungsten probes. The Tegam 871 digital thermometer in conjunction with Kapton p08508-86 K thermocouple probes with tip diameter 0.254 mm was placed on contact pads to measure the channel temperatures.

3.3 Results and Discussion

Etching the <100> oriented silicon wafers in KOH (45% by volume) produced wells with 54° angle sidewalls. Since the substrate was <100> oriented, the chemical wet etching produced the channels anisotropically with low aspect ratios. As a result, the channel geometry was trapezoidal as shown in Figure 3.2. Several channel configurations were fabricated with a width between 50 to 456 μm, depth between 35 and 350 μm and length between 6 and 19 cm. The separation distance between the channels was varied such that the entire microheater fitted in a $1cm^2$ area. Figure 3.3 shows the fabricated heater with two contact pads.

The resistance, R, of the circuit element can be computed as:

$$R = \rho \frac{1}{t}\left(\frac{L}{W}\right) \tag{3.1}$$

Where ρ is the resistivity of conducting material, t is the thickness of the conducting material, L is the overall length of channel, and W is the width of channel.

The different channel configurations shown in the Table 3.1 were fabricated on a single wafer to find an optimal heater configuration. Three different thicknesses, 1 μm, 3μm and 5μm, of conducting films were deposited on the channels. The channels with thickness of 5μm failed to be patterned in the standard UV lithography process. Due to the excessive thickness of the conducting film, there was not enough separation space between the mask and the wafer. This resulted in incomplete wafer pattern.

Table 3.1 Experimental and Theoretical Resistances of the Microheaters of Different Dimensions

Heater Type	W [μm]	L [cm]	Resistance with 1μm metal film	
			Rt[1] [Ω]	Re[2] [Ω]
A	456	6.7	3.9	5.8
B	300	6.0	5.3	14.2
C	456	18.7	10.9	21.0
D	50	6.0	31.8	40.0

[1]Rt is a computed resistance.

[2]Re is an experimental resistance.

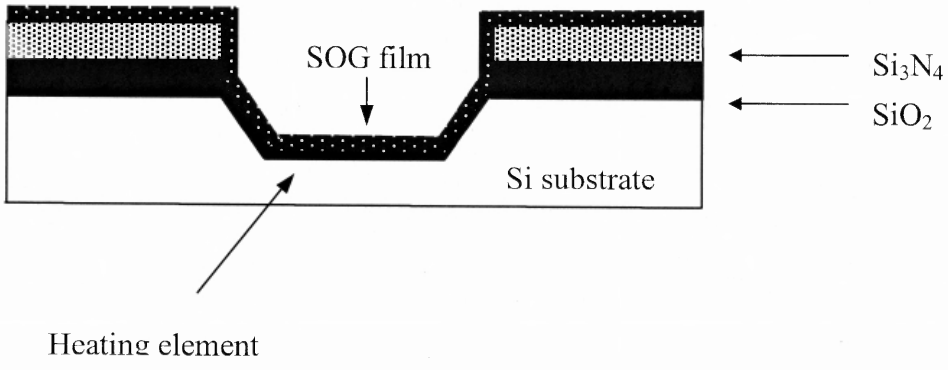

Figure 3.2 Cross section of the etched channel of microheater.

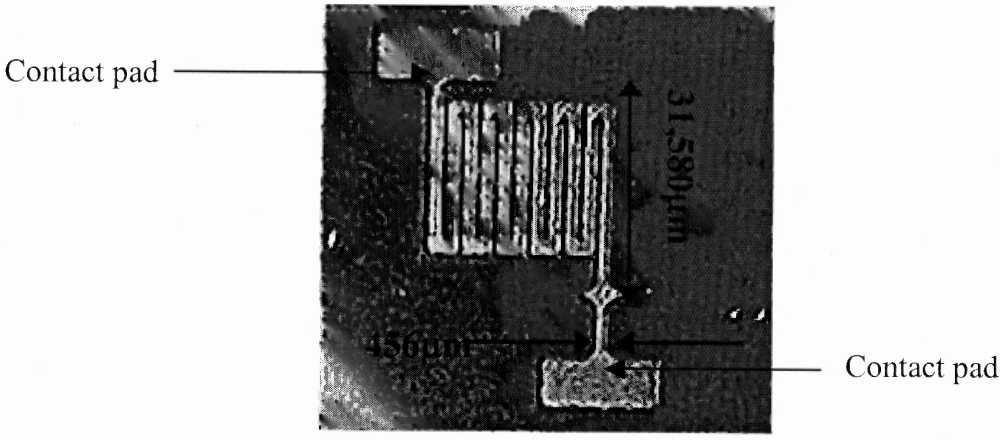

Figure 3.3 Photograph of the heated channels on silicon wafer (top view).

Theoretical resistance, Rt, could be calculated based on known resistivity, thickness of conducting material and its dimension. The experimental resistance, Re, are shown on Table 3.1. As predicted by Equation 3.1, the resistance of the heaters with 1μm metal film was higher than those with 3μm thick metal. Similarly, between A and C, C had higher resistance because it was longer. Although aluminum based alloys have been the metalization of choice for silicon IC technologies, it suffers from electromigration [79]. Electromigration can lead to the electrical failure of metallic conductors in relatively short times, reducing the circuit lifetime to an unacceptable level [69]. The problem occurs when long skinny leads of aluminum carry high currents over long distances. The current sets up an electric field at the lead that decreases from the input side to the output. Also, heat generated by the flowing current sets up a thermal gradient along the aluminum lead.

The heating characteristics of microheater at different voltages as a function of time were studied. The initial temperature was between 23 and 25 °C for all the heaters. The temperature profile of heater A with 15, 30, and 36 volts across it are shown in Figure 3.4. It took an average 10 to 20 seconds to reach the maximum temperature. It took only less than 5 seconds to cool down to its initial temperature. The microheaters cooled faster than they heated up. This was because the wafer was exposed during these tests and was prone to heat loss while there was only one heating source, which slowed down the heating rate. In the In all cases, temperature stabilized in less than 30-seconds. Table 3.2 shows the maximum temperatures attained for different heater configurations. As shown in Figure 3.4 and Table 3.2, the maximum temp. in excess of 350 °C could be

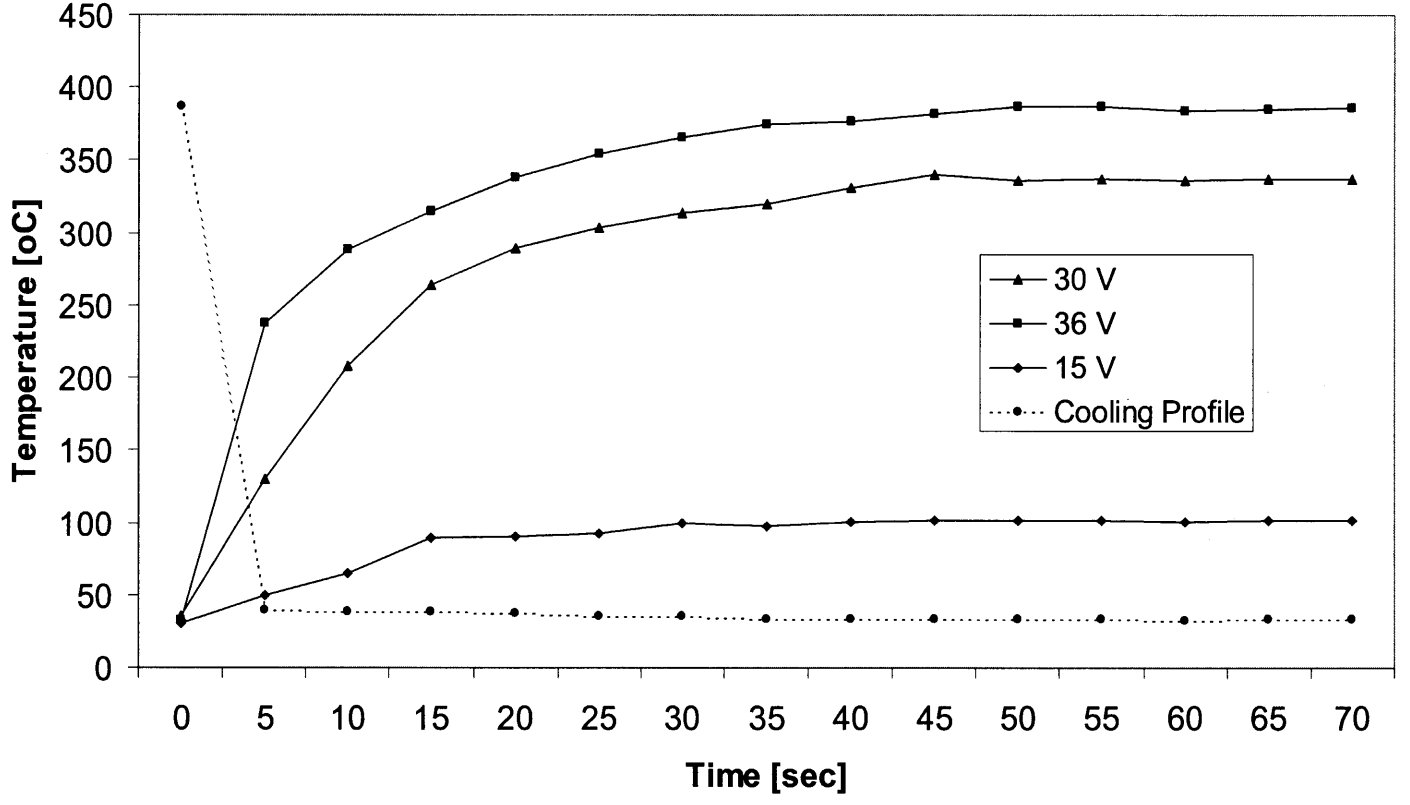

Figure 3.4 Temperature profile of heater type A with 1μm metal film when different voltages were applied.

achieved with approximately 36V. It should be noted that higher temperature could be attained by applying higher voltage or changing film thickness.

Table 3.2 Maximum Temperature Measured [°C] for Different Metal Heaters at 40 Volts

Heater type	METAL	METAL	METAL With SOG
	Metal (Al)	Metal (Al)	Metal and SOG
Thickness	1μm	3μm	1.7μm †
A	387	256.6	130.8
B	246.8	110.0	52.0
C	137.1	90	41.2
D	86.0	58.4	30.9

†Total thickness of metal and SOG (Metal is 1μm thick and SOG is 0.7μm thick).

The amount of power that is transferred to the load from the source will be at its maximum when the resistance of the load matches the internal resistance of the source. When the load resistance, R_L, is greater than the internal source resistance, R_i, the load voltage is higher but the load current is reduced. When R_L is smaller than R_i the load current is higher but the load voltage is reduced. Only when R_L and R_i are equal is the product of the load voltage and the load current is at the maximum value. Since power is the product of voltage and current, this is the point of maximum power transfer. To transfer maximum power to the aluminum heating element, one needs to match the source resistance to that of the load resistance. The resistance of 1 μm thick metal was higher than that of 3 μm thick metal. However, the maximum temperature output observed for 1 μm metal was higher than 3 μm metal due to the matching of the source

resistance to the metal resistance. So, while designing the heating element, one needs to mach the source resistance to that of the heating element.

3.3.1 Comparison with heater made by boron implantation

The 2nd set of heaters was made by low dose boron implantation. The resistance was a function of dopant concentration. The wafers were annealed at 400°C in a forming gas, Argon. The annealing brought some of the dispersed dopant ions closer to the surface, thus forming a uniform conductive layer. Inadequate annealing could result in a bulk of the implanted ions being distributed too deep into the substrate to contribute to conductivity. Two different implantation regimes were tried out. Furthermore, in an effort to improve heating characteristics, each was subjected to two different anneal times.

In order to arrive at the proper energy and dose of the boron source, the concentration following the annealing was simulated using a computer program called SUPREME III (Stanford University Process Emulator). This determined the depth of the penetration of the boron atoms. For the first run, implantation energy was 80 keV at a dose of 1×10^{14} atoms / cm^3. For the second run, implantation was at a higher dose, 2×10^{15} atoms / cm^3, and at 100 keV. After annealing (dopant activation), boron ions come to rest at various depths in the wafer. They are centered about a depth called the projected range at which diffusion depth can be predicted and fall of in density. The conditions utilized for the initial implantation schedule are:

Implantation energy = 80 keV

Implantation dose = 1×10^{14} atoms/cm^2

Anneal = 40 minutes

Additional anneal = 20 minutes

and the simulation is presented in Figure 3.5.

Since the measurement result obtained from this wafer were not very favorable, secondimplantation schedule involving a higher dose and energy was also tried out. The conditions used in the implantation are:

Implantation energy = 100 keV

Implantation dose = 2×10^5 atoms/cm^2

Anneal = 20 minutes

Additional anneal = 20 minutes

The simulation results are presented in Figure 3.6. As can be seen, this results in a higher implanted concentration of dopant and a much more uniform distribution upto a greater depth within the substrate following annealing.

The resistance of the heaters was calculated based on Equation 3.1 from the resistivity of the material if the thickness of conducting film and the L/W ratios are known. For the boron-deposited wafer, the resistivity could be calculated based on mean boron concentration and the depth of the boron layer. The resistivity for this concentration was obtained from literature [80].

The sheet resistances after boron implantation were measured. The computed and measured total resistances are listed in Table 3.3. The resistances with boron doping were much higher than those obtained by metal deposition. For the initial implant (80 keV, 1×10^{14} / cm^2, 40 minutes anneal at 900 °C), the concentration was 5×10^{19} / cm^3 at a depth of 0.4 μm with ρ of 1.8×10^{-3} Ω - cm. For the second implant atom (100 keV, 2×10^{15} / cm^2, 20 minutes anneal at 1050 °C), the concentration was 1×10^{20} / cm^3 a depth

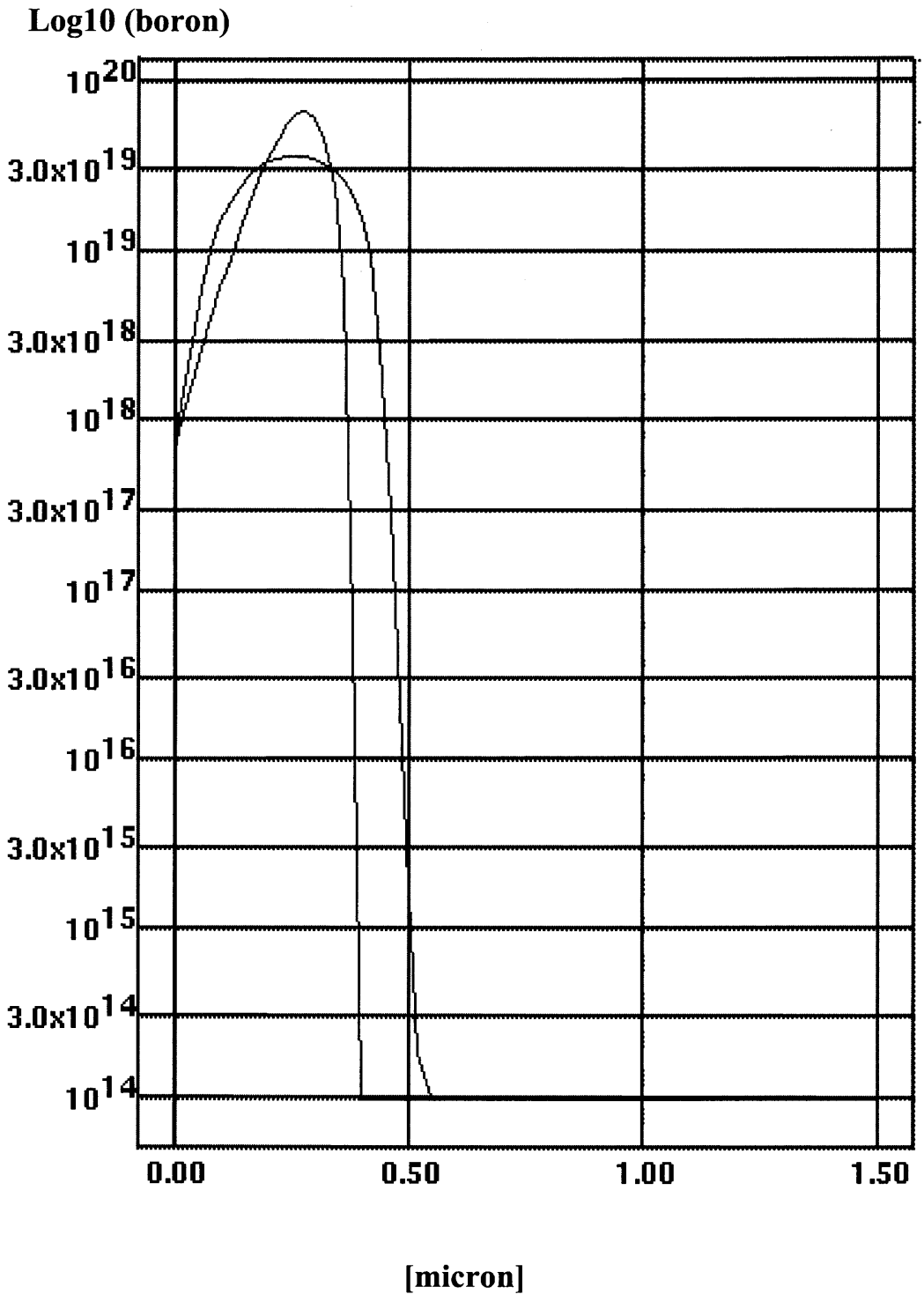

Figure 3.5 Boron concentration profile in silicon after implantation and annealing.

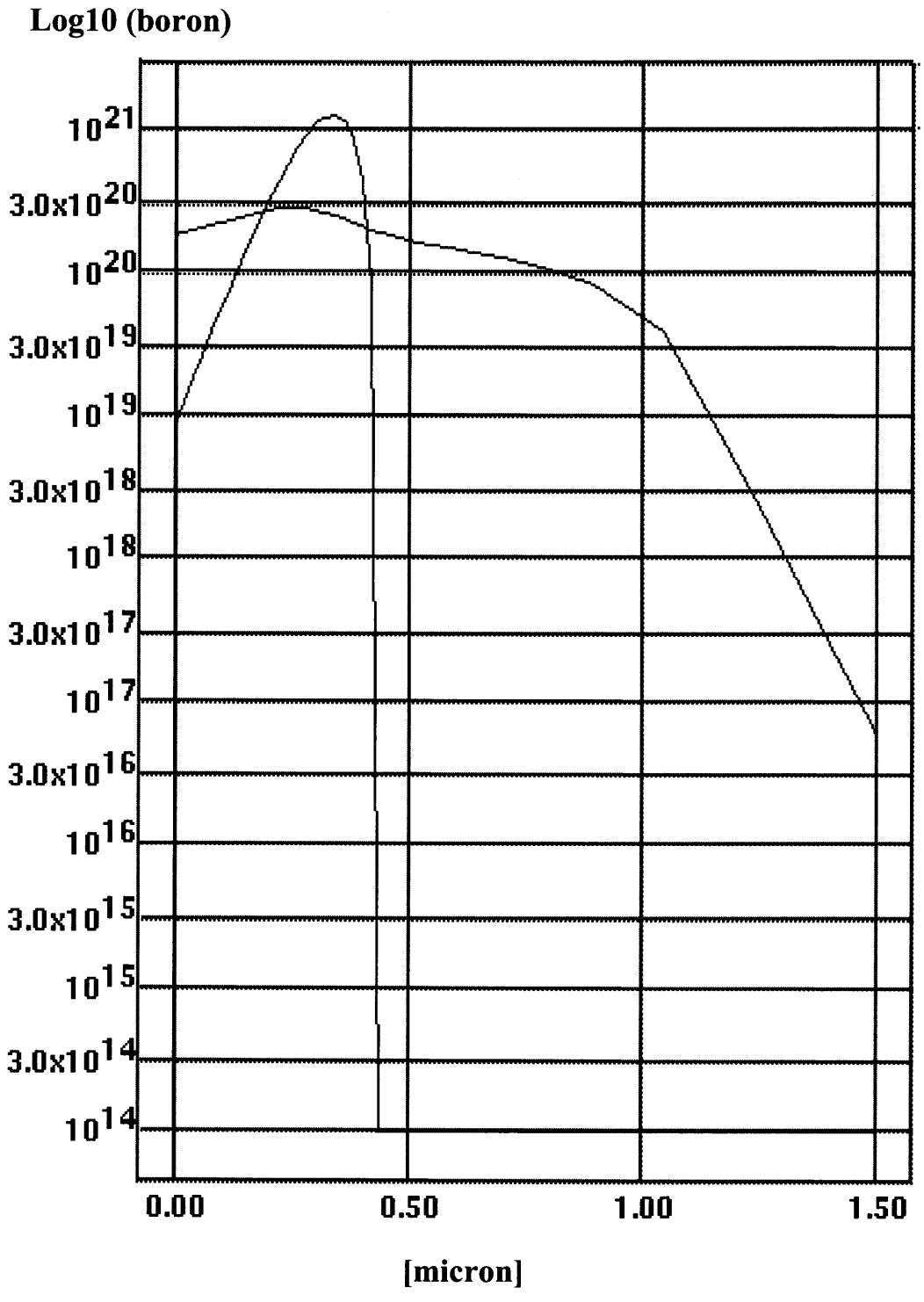

Figure 3.6 Boron concentration profile in silicon after implantation and annealing: alternative implantation regime.

of 1 μm with ρ of 5 x 10^{-4} Ω - cm. The second scheme brought about an order of magnitude decrease in the resistance of the channels. However, even this was a very high resistance suggesting that even higher dose of doping is necessary probably in the range of 10 x 10^{19}/ cm^3 to 10^{21} / cm^2. However, such heavy doping increases the fabrication cost a hundred to a thousand times.

Table 3.3 Calculated and Measured Resistances and Measured Power for Individual Channels

Heater Type	Implant at 80 keV, 1 x 10^{14} / cm^2, 900°C			Implant at 100 keV, 2 x 10^{15} / cm^2, 1050 °C		
	Rt (kΩ)	Re (kΩ)	Power (W)	Rt (Ω)	Re (Ω)	Power (mW)
A	6.0	0.54	0.3	665	66.7	41.7
B	18.4	1.95	1.2	2000	125	78.1
C	156	25.5	15.9	17400	1600	1000
D	131	∞	∞	14600	73	45.6

Table 3.4 shows the maximum temperature attained by different fabricated heaters under different annealing conditions. It shows that annealing beyond 20 minutes did not increase the maximum attainable temperature by the heaters.

Figure 3.7 shows the temperature rise in the boron-doped wafer as a function of time. For instance, the channel type A with a metal heater could attain temperature up to 387 °C, while the maximum temperature attained with boron doping was 67.3 °C. However, the heating profile of the doped was similar to the heaters with the metallic layer. In the conductivity depended on the dopant concentration.

Table 3.4 Maximum Temperature Measured [°C] for the Boron Implanted Heaters at 40 Volts

Heater Type	BORON Implanted, Annealed			
	80 keV $1x10^{14}/cm^2$ 40 minutes annealing	80 keV $1x10^{14}/cm^2$ 60 minutes annealing	100 keV $2x10^{15}/cm^2$ 20 minutes annealing	100 keV $2x10^{15}/cm^2$ 40 minutes annealing.
Boron Diffusion Depth	0.3 μm	0.4 μm	1μm	1.2 μm
A	32.8	36.6	64.3	62.0
B	25	26.1	44.0	38.1
C	26.7	26.7	26.0	27.3
C	25	25.9	40.3	40.4

3.3.2 Effect of Glass Coating

It is expected that in many applications, the heater would be coated with some other material such as glass or polymer. For example, those used in electrophoresis and chromatography require glass-based surfaces because of the ease of chemical modification using organosilanes [81]. Since organic polymers have low adhesivity for silicon or metal, a layer of glass can be used on the substrate for modification. Hence, a coat of Spin-on-glass (SOG) was applied on the channels to see how it effected the

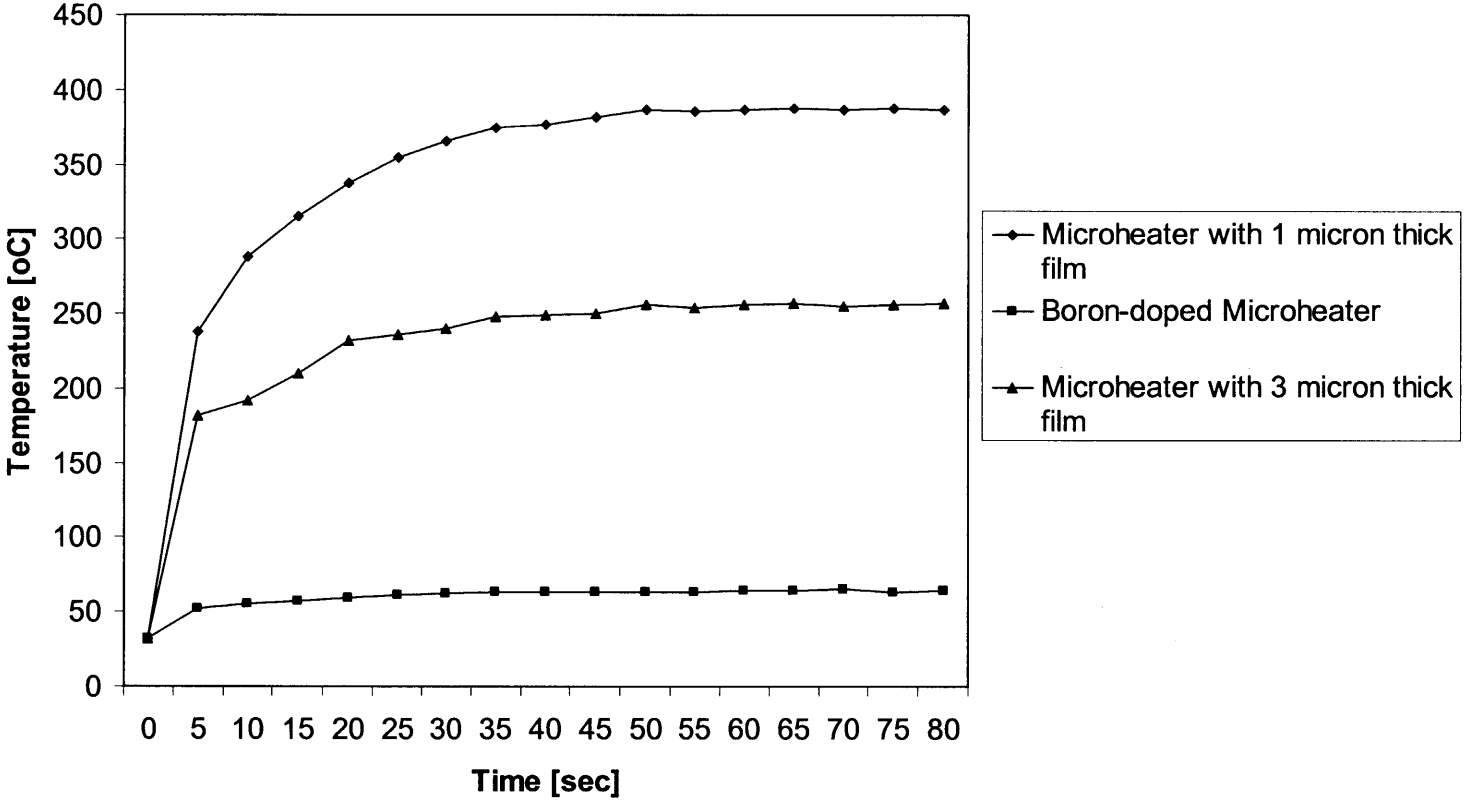

Figure 3.7 Temperature characteristic of microheater type A with 1 and 3 μm aluminum film and by boron doping at 100 KeV at a dose of $2x10^{15}/cm^3$. The voltage applied was 36V.

temperature characteristics. The thickness was controlled by the speed of the spinner. For the six inch wafers, 4 ml of SOG was applied at 2000 RPM for a period of two seconds. This achieved a glass thickness of 1μm. This was followed by hard plate baking at 80°C, 150°C and 250°C for 40 seconds each. Then the wafers were cured in a furnace at 425°C for 60 minutes.

The rise in temperature as a function of time with the spin-on glass coating are presented in Figure 3.8 at an applied voltage of 43 V. In all cases, the temperature stabilized in less than 10 seconds. As expected, the glass film served as a barrier to heat transfer and the maximum temperature attained was significantly lower. At an applied voltage of 36, temperatures was as high as 390 °C in the absence of the glass coating, whereas the maximum temperature at an applied voltage of 43 with spin-on-glass was 120 °C.

3.3.2 Microheater under Repeated Cycles

Stability of heater to alternate heating and cooling was studied by applying a series of repeated voltage pulses. Series of 2 seconds, 30 V pulses were applied to heater A, and the current was measured. This was repeated every two minutes for five hours. The results are shown in Figure 3.9. The heater was able to reach a constant current of 1.6 A for each voltage pulse. We also demonstrated that the temperature reached as high as 100 °C within a pulsing period of two seconds. The resistance of the heater did not change during the 148 cycles performed here. In another set of experiments, the heater was cycled for seventeen hours (overnight). The current stayed the same even after 486 cycles.

The precision was calculated by determining relative standard deviation or RSD:

$$RSD\% = \text{Std. Dev.} / \text{Mean Conc.} \times 100 \quad (3.2)$$

RSD for 148 cycles was 0.620 %. This demonstrated the ruggedness of the microheater, under widely ranging voltage application.

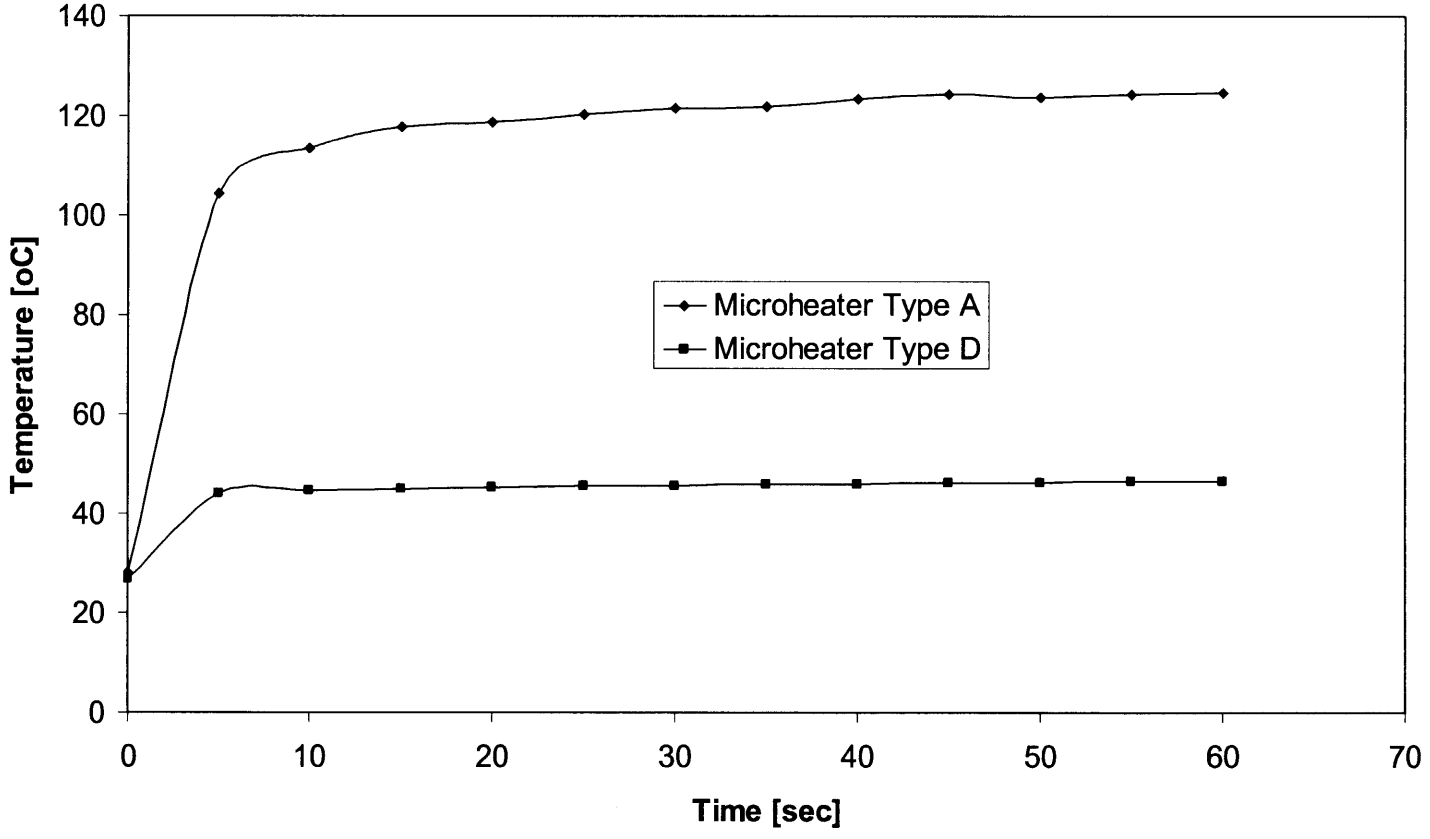

Figure 3.8 Temperature characteristics of 1 μm metal deposited microheater type A and D with Spin-On-Glass.

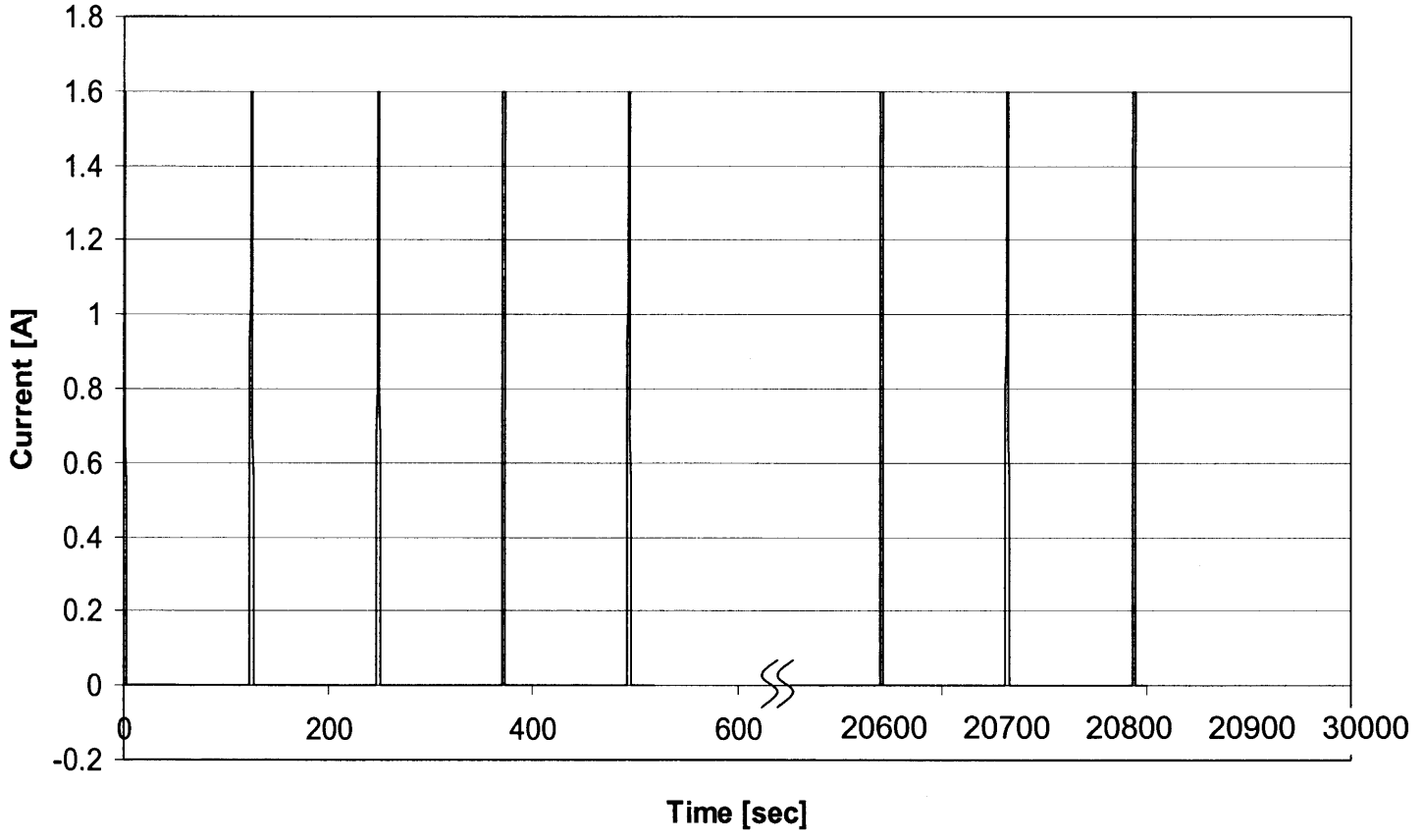

Figure 3.9 Current profile for each voltage pulse to the heater type A; 30 V pulses were applied every 2 minutes for a period of 2 seconds.

CHAPTER 4

A MICROFABRICATED MICROCONCENTRATOR

4.1 Introduction

The environmental monitoring requires the measurements of pollutants at very trace concentrations (ppm to ppt) because even at such low concentrations they pose a threat to human health and the environment. Continuous, on-line determination of the trace level of organics in aqueous or gaseous matrix presents many challenges. A variety of conventional laboratory based analytical techniques are used for pollution monitoring. Currently, gas chromatographs, mass spectrometers and Fourier transform infrared (FTIR) are the most commonly used instruments [82-88]. These techniques have excellent figures of merit in terms of sensitivity, detection limit and other performance characteristics [88-91]. However, they are relatively large, expensive and do not lend themselves to easy portability.

The increasing needs for inexpensive, small monitoring devices have added new impetus to miniaturize of chemical analysis systems. It is well known that the miniaturization offers functional and economical benefits such as the reduction of the sample size, decrease in reagent consumption and inexpensive mass production [92]. The advancements in thin-film microfabrication technology over the past few years have opened a wide range of possible microsensor designs. Micromachining processes, particularly anisotropic and plasma etching, and the sacrificial layer method make possible the construction of three-dimensional structures. It is feasible to employ these techniques to produce chemical and gas sensors to meet the desirable sensor properties.

Low energy consumption devices can be produced at modest cost [93,94]. The high degree of reproducibility and relatively small size of these sensors enhance both performance and the potential for practical applications.

Development of several microfabricated sensors has been reported [94,95]. Tin-oxide-based sensors have been widely used in gas sensing [95-97]. An important environmental application is the detection of low concentration toxic gases (i.e., CO, NO_2, O_3 etc.). SnO_2 films are commonly used as gas sensors due to their high sensitivity to different gases, low production cost and the ease of use. Surface acoustic wave (SAW) sensors are another widely used class of environmental sensors [98,99]. It offers very high detection sensitivity for chemical sensing. A coated SAW device acts as a chemical sensor by adsorbing analytes on its surface. A mass loading on the surface results in a change in propagation velocity and a corresponding phase shift. Schottky-diode-type sensors have also been used in gas sensing [100]. When an analyte molecule diffuses toward the interface between the metal and the insulting layers of a diode, the height of the Schottky barrier diminishes. This leads to a change in either the forward voltage or the reverse current of the diode, forming the mechanism of the gas or chemical vapor diode. Many chemical species can be detected using electrochemical sensors. An example of the solid electrolyte electrochemical sensor for gas sensing is the ZrO_2- based high-temperature oxygen sensors [101]. This sensor is operated at 650°C in order to ensure the ionic conductivity of ZrO_2, and the amount of energy required to heat the sensor is relatively large.

Micromachined, micro gas chromatographs have also been developed [102,103]. GC columns have been etched on silicon, and diaphragm based injection valves have

been developed [104]. Micromachined thermal conductivity detector has been successfully made and is currently available commercially. The potential to use a whole micromachined GC as a sensor is also an attractive idea.

In principle, sensors can provide real-time (or near real-time), on-line measurements. Furthermore, it is desirable that the senors be completely automated, and not require additional chemical reagents or sample preconditioning. Figures of merits necessary for different measurements are high sensitivity, selectivity, reproducibility, short response time and long-term stability [109]. The limited successes of microsensors are due to the inability to meet some of these requirements. In trace measurements applications such as in environmental monitoring and chemical vapors detection, the biggest draw back has been the low sensitivity and high detection limit of the sensors [105].

One way to enhance sensitivity in any measurements is to provide some kind of preconcentration. Sorbent trapping in air sampling, solid phase extraction and SPME are common examples of preconcentration [106,107]. This allows a larger amount of analyte to be concentrated and then released into the detection device or sensor. Larger sample throughput in terms of mass of analyte per unit time results in a high signal to noise ratio. These ideas have been used in different conventional measurements. Over the last few years, we have reported the use of a microtrap as concentration cum injection device for continuous monitoring of organics in a gas stream by GC, mass spectrometry, or a non-methane organic carbon analyzer [108-111]. The microtrap is a small sorbent trap that is put on-line. Sample passes continuously through it, and periodic electrical heating releases the adsorbed gases as a "concentration pulse", which serves as an injection for

the detection system. Its small size allows it to be cycled at high frequency, and the preconcentration effect allows ppb level detection.

It is envisioned that the sensitivity of a microsensor can be enhanced by providing on-line preconcentrator. The objective of this research is to micromachine a concentrator (referred to as the microconcentrator) on a silicon substrate that can be integrated with a sensor or a micromachined GC to enhance the signal to noise ratio. Basically, the microconcentrator is a miniaturized sorbent trap fabricated on a microchip. It is to be fabricated on silicon substrate so that a sensor can be integrated on the same chip. The microconcentrator is put on-line with the sample stream, and is operated at a fixed frequency. In principle, the microconcentrator is similar to the microtrap for GC and MS described above. It is composed of microchannels etched in silicon. The channels are lined with a microheater for in-situ heating. The preconcentration is done on thin-film polymeric layer deposited above the heater in the channel. Rapid heating by the channel heater generates "desorption pulse" to be injected into a detector or sensor. This chapter presents the development of characterization of the microconcentrator.

4.2 Experimental Section

4.2.1 Fabrication

4.2.1.1 Flow Chart for Fabrication of the Microconcentrator: The following shows a flow chart of the entire processing to fabricate the microconcentrator (The Traveler is shown in Appendix A).

Silicon Wafer

↓

Steam oxidation to grow oxide

↓

Deposition of LPCVD nitride

↓

Photolithography to pattern the nitride

↓

Reactive Ion Etching (RIE) of nitride and oxide

↓

Stripping photoresist

↓

Wet etching of the silicon

↓

Sputtering of the metal

↓

Photolithography to pattern the metal

↓

Wet etch the metal

↓

Stripping the photoresist

↓

Spin coating of the spin-on-glass (SOG)

↓

Spin coating of the polymer

↓

Bonding with the quartz wafer

4.2.2 Process

The materials used for this microconcentrators were <100> oriented, 6-inch, p-typed (boron doped), single side polished silicon wafers, with a thickness of 575 μm and a resistivity of 10-25 Ω-cm. The chip layout was done on a Sun Sparc workstation using IC tool in Mentor Graphics (Wilsonville, OR). All fabrications were done at the New Jersey Institute of Technology Microelectronics Research Center cleanroom. Figure 4.1 shows the step by step processing of the wafer and its cross sectional view after each step.

The detail process flow is described in Section 3.2.1. The first step was steam oxidation of the wafers to grow the oxide layer. This was followed by LPCVD to deposit the nitride layer. Then the wafers with 2000Å thick oxide and 1550Å thick nitride were patterned using standard UV lithography. The patterned wafers were etched using Reactive Ion Etching (RIE). After this, anisotropic etching with KOH was performed at 95 °C for 3.5 hrs at an etch rate of 1.66mm/min. Etching the <100> oriented silicon wafers in KOH (45%) produced wells with 54° angle sidewalls. Since the substrate was <100> oriented, the chemical wet etching produced the channels isotropically with low aspect ratios. As a result, the channel geometry was trapezoidal as shown in Figure 4.2. Several channel configurations were fabricated with a width between 50 to 456 μm,

Silicon Wafer

↓

Steam oxidation to grow oxide

↓

Deposition of LPCVD nitride

↓

Photolithography to pattern the nitride

↓

Reactive Ion Etching (RIE) of nitride and oxide

↓

Stripping photoresist

↓

Wet etching of the silicon

↓

Sputtering of the metal

↓

Photolithography to pattern the metal

↓

Wet etch the metal

↓

Stripping the photoresist

↓

Spin coating of the spin-on-glass (SOG)

depth between 35 and 350 μm and length between 6 and 19 cm. The separation distance between the channels was varied such that the entire microheater fitted in a $1cm^2$ area.

Sputtering used deposition of metal in the channel by sputtering to form a conductive layer. The metal source used in this study was aluminum alloy, which was 99% aluminum, the rest being silicon and copper.

Then the microconcentrators were coated with Spin-On-Glass (SOG) since microconcentrator require glass-based surfaces because of the ease of chemical modification of glass surfaces using organosilanes. Since organic polymers have a low adhesivity for silicon or metal, a coat of glass was specially applied on the channels by spinning them over the surface of the wafer. SOG materials consist of polysiloxane polymer, and, upon heat treatment, become SiO_2-like in character. The SOG (Honeywell) was applied on Si wafers by using the spinner. The thickness was controlled by the speed of the spinner. For the six inch wafers, four ml of SOG with 2000 RPM for 2.0 seconds was applied to achiever approximately 1 μm followed by hard plate baking at 80 °C, 150 °C and 250 °C for 40 seconds each hot plate. Then the wafers were placed in the furnace for curing process at 425 °C for 60 minutes.

Thin films of commercially available gas chromatography stationary phase, OV17 (polymethyl-phenyl-phase) were deposited on the microconcentrator using a spin coating at 2000 rpm for 20 seconds to form an adsorbent layer. By adjusting spin-coating conditions, the thickness of the polysilane was varied. Then the wafers were placed in the oven for baking at 120 °C for 48 hours.

WaferGrip (Dynatex, Santa Rosa, CA) was used to bond patterned Silicon and quartz glass wafers. WaferGrip is an advanced composite film adhesive engineered to

securely bond wafers and other substrates during dicing, grinding and polishing. WaferGrip is a heat activated adhesive of uniform thickness. Using Wafer Bonder, the adhesive layer of WaferGrip is compressed on a substrate under vacuum. Adhesive on a polyester backing or as a film on release paper may be used. With its high shear strength, WaferGrip secures devices as small as 5 mils square and still maintains adhesion for maximum feed rates. In Figure 4.3, the cross section view of the microconcentrator after the all processes were completed is presented.

4.3 Cross Sections

A. The Silicon wafer was p-type. 1500 Å steam oxide was grown on the wafer.

B. A 2000 Å thick silicon nitride was deposited

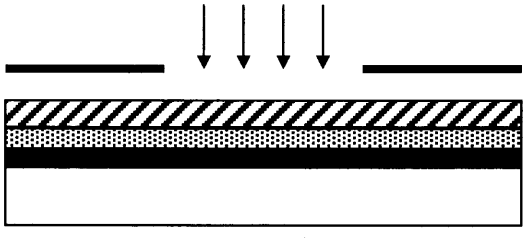

C. Photoresist was then deposited and Si_3N_4 and SiO_2 were patterned.

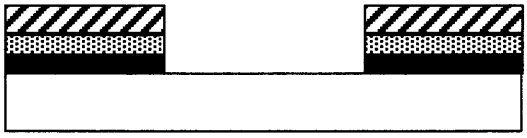

D. Si_3N_4 and SiO_2 were RIE etched

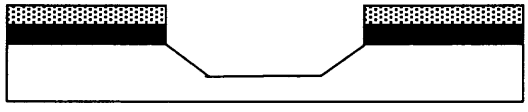

E. Photoresist was stripped and KOH wet etch was then done.

F. Metal was sputtered.

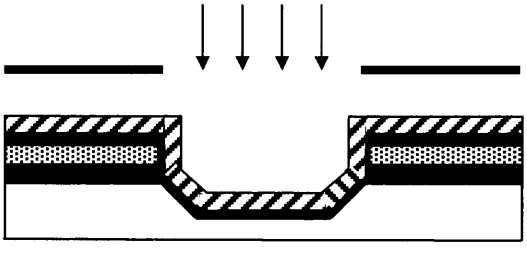

G. Photoresist was then deposited and was patterned.

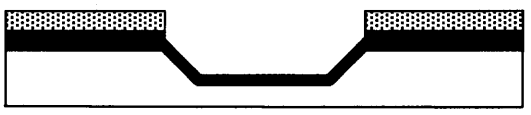

H. Metal was patterned using metal mask as shown above.

I. Spin-on-glass was coated.

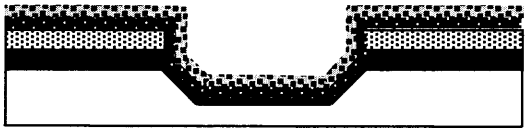

J. Polymer was coated.

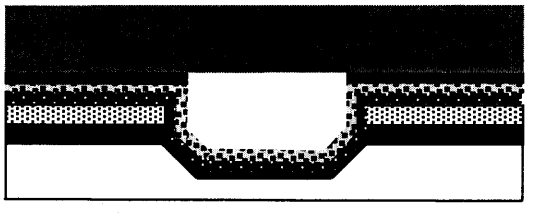

K. Bonding with quartz wafer using WaferGrip.

Figure 4.1 Cross sectional view after each step.

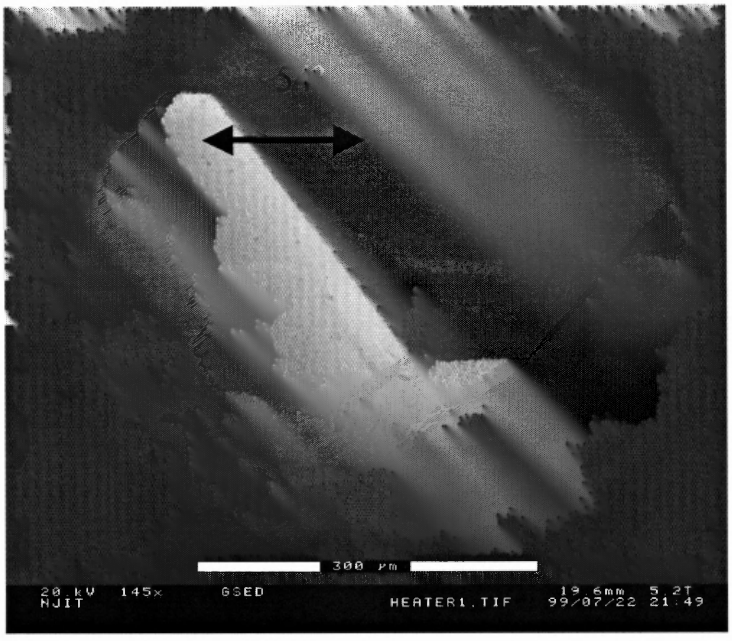

Figure 4.2 SEM image of the anisotropically etched channel of the Microconcentrator.

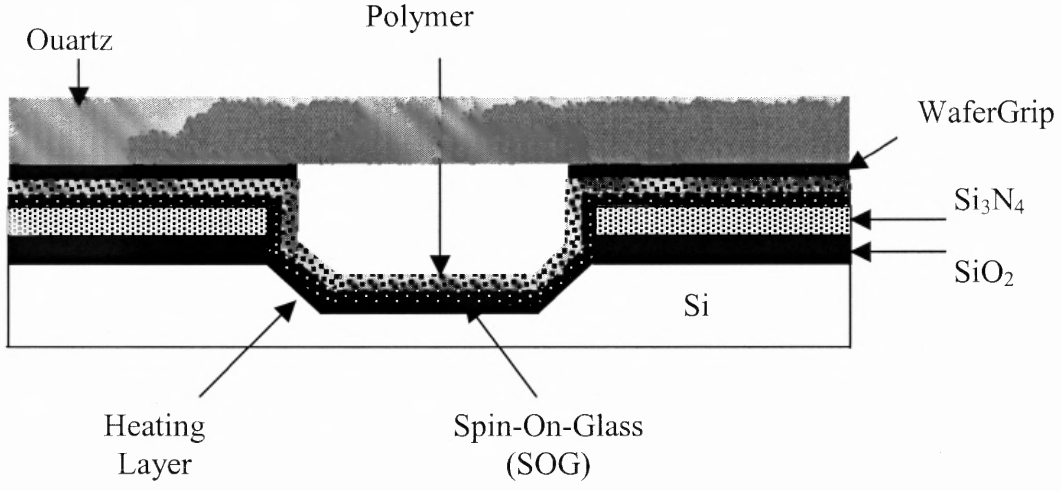

Figure 4.3 Cross section of the etched channel of microconcentrator.

4.2.3 Experiment Set-up

Once all process steps were completed, microconcentrator was tested by interfacing with Flame Ionization Detector (FID). The experimental system used in this study is shown in Figure 4.4. A SRI Instrument model 8600/9300 portable GC equipped with a flame ionization (FID) detector was used for analysis. In some tests, a 0.53 mm ID, 30 m capillary column (DB-624, J&W Scientific) was used. Standard gases such as air, nitrogen, and hydrogen were purchased from Matheson Co., NJ. Nitrogen flow was used as the striping gas and the flow rate was set to 11 ml/min. A steady toluene stream was generated by diffusing a controlled amount of the analyte from diffusion capillary into a flow of N_2. The toluene liquid was placed in a melting point capillary of 0.1mm diameter. The sample diffused up the capillary tube onto a flow of N_2. Toluene and benzene vapors were prepared by a headspace technique. A microprocessor was used to control the interval, and duration of the electrical pulses to the microconcentrator. The toluene vapors passed along with a stream of air, and toluene was adsorbed by the microconcentrator. The preconcentration was done on thin-film polymeric layer deposited in the channel. After a sufficient time has elapsed, three minutes, a pulse of electric current was applied to the micro-concentrator to desorb the trapped organics. Rapid heating of the conductive layer caused the "desorption pulse" to be injected into the detector. The use of microconcentrator enhanced the sensitivity by generating series of pulses.

Software used for data collection was the Peaksimple Data System supplied by SRI Instruments. It provided precise temperature controls for the GC oven and its

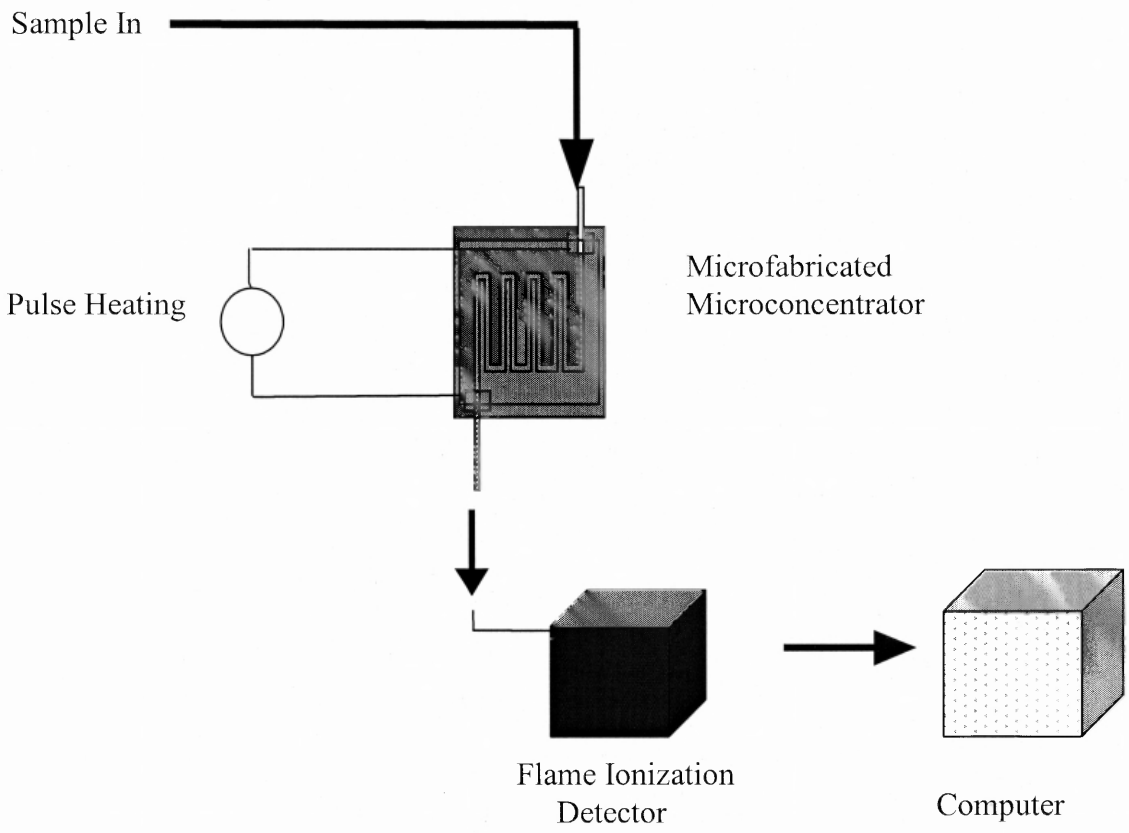

Figure 4.4 Schematic diagram of the experimental system.

detector. Calibration, real-time qualitative/quantitative analysis, documentation of analytical results, and report output were also controlled and handled by this date system.

4.3 Results and Discussion

4.3.1 Heating Characteristics of the Microheater

The key component in the microconcentrator is the heating element embedded in the channel. The heating characteristics of the channel heater of the microconcentrator were studied.

The temperature of the microchannel was measured using a 50 μm thermocouple. Typical temperature profile as a function of time is plotted in Figure 4.4. The temperature depended upon several factors such as heater design, applied voltage etc [112]. For the heater presented here, temperature as high as 330 °C could be reached in less than 10 seconds. The SOG provides a resistance to heat transfer and the maximum temperature was only 120 °C. It should be noted that the thermocouple has slow response, and the real heat-up rate could be somewhat higher. Detailed heating characteristics of such thin-film heater have been presented elsewhere, and the heater stability during multiple cycling has been demonstrated [113].

4.3.2 On-line Microconcentrator

The microconcentrator was put on-line with the sample stream. The gaseous sample containing the analyte was introduced into the detector through the microconcentrator. The analytes were trapped in the polymer film and could be thermally desorbed by electrical heating. The desorption of the microconcentrator was achieved by resistive heating using an electrical current pulse. Rapid desorption was essential for producing a

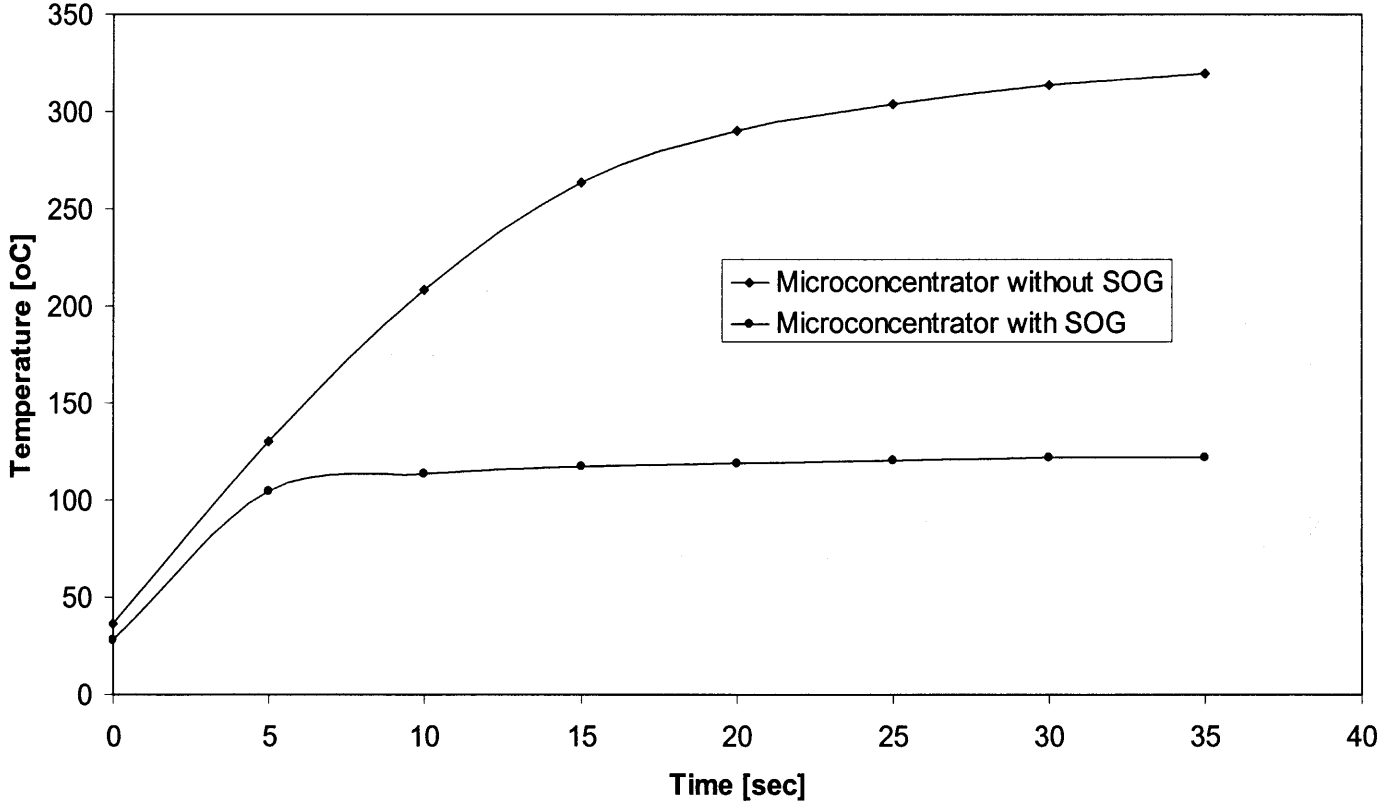

Figure 4.5 Temperature characteristics of 1 μm metal deposited Microconcentrator with and without Spin-On-Glass.

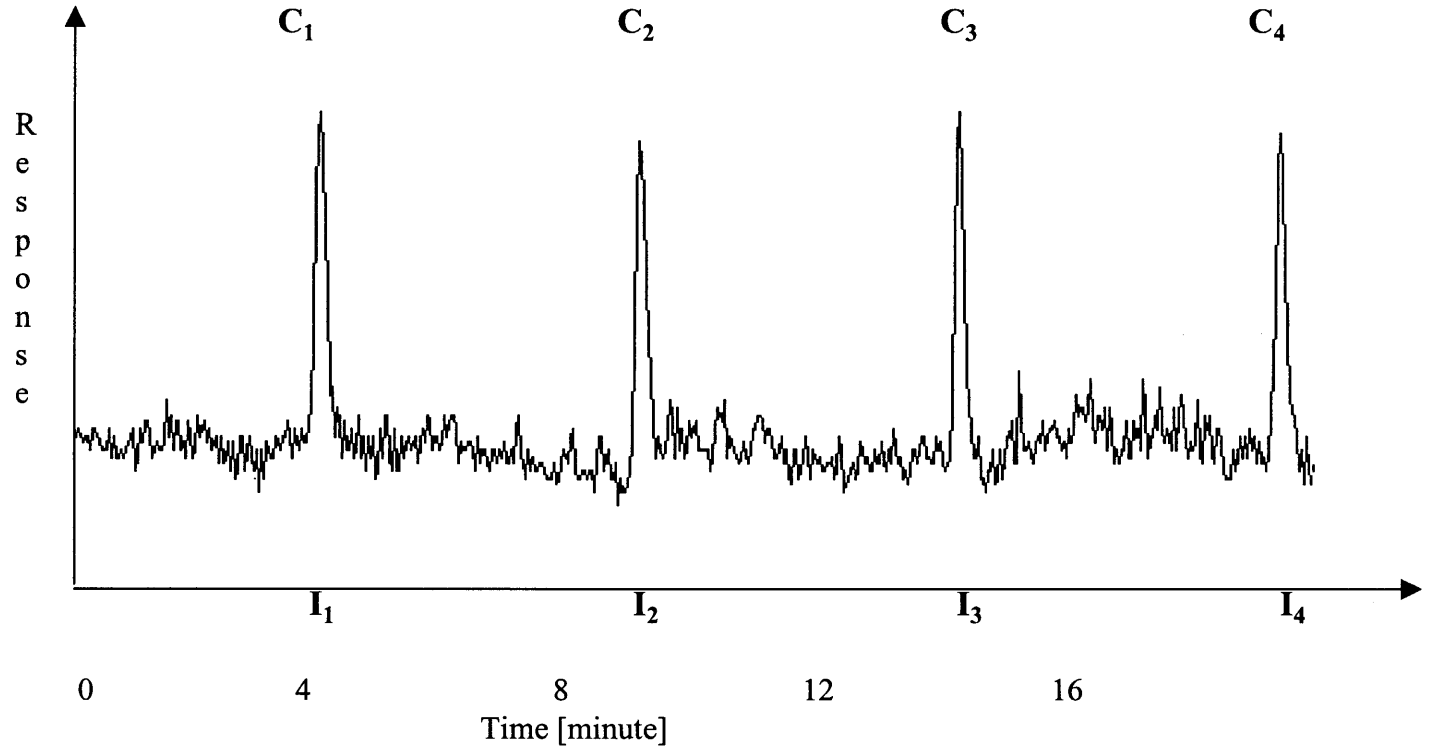

Figure 4.6 Continuous monitoring of a stream containing organics. Corresponding to each injection I_1, I_2, I_3..... a response C_1, C_2, C_3....was obtained.

sharp concentration pulse to provide high throughput in terms of mass of sample per second. The mode of operation for continuous monitoring is that electrical pulses, or injections were made at fixed intervals of time and corresponding to each injection, a signal pulse was obtained. Continuous monitoring using the microconcentrator is demonstrated by monitoring a stream of organic vapors. As shown in Figure 4.6, microconcentrator generated a series of signal pulses corresponding to a sequence of injections. Reproducibility in terms of peak height was excellent, and injection pulses could be continued indefinitely.

Both adsorption and desorption processes play important roles in the on-line microconcentrator operation. In a previous study, the effect of capacity factor in conventional packed tube microtrap was described [114]. Similar ideas are applicable here. The capacities of adsorption in terms of analyte breakthrough, and desorption efficiency are important issues. Because of its small dimensions, only a small amount of polymer could be coated inside. Consequently, the microconcentrator had inherently low capacity and was prone to breakthrough.

The breakthrough characteristics can be studied from the peak shape. The sample flowed continuously through the microconcentrator. When the microconcentrator was heated, a desorption peak was observed. The analytes were re-adsorbed in the microconcentrator as it cooled. This lowered the base line into the negative territory appearing as a negative peak. As the sample began to breakthrough, the detector response increased back to the base line. The width of the negative peak has been shown to equal to the breakthrough time measured by frontal chromatography [109]. The desorption generated a positive concentration profile while the immediate sample

readsoprtion generated a negative one. Thus, a microconcentrator peak contained a positive and negative part as shown in Figure 4.7. The time interval AD in Figure 4.7 is the time taken by the sample to migrate through the microconcentrator. This is denoted as

$$t_b = (k + 1)\, L/u \qquad (4.1)$$

Where L is the length of the microconcentrator, u is the flow-rate of the sample and k is the capacity factor of sample in the microconcentrator stationary phase. As capacity factor, k, increased, t_b increased, the negative peak became shallow and appeared to merge with the baseline so that the peak resembled a conventional concentration spike without a negative profile. Figure 6 represents a low capacity microtrap with a very thin-film coating where the negative peak is pronounced. Whereas, Figure 4.6 shows the response of a higher capacity microconcentrator with relatively thicker polymer film and without a negative profile. A microconcentrator with a higher capacity factor allowed longer breakthrough time, and generates peaks without a negative part.

The microconcentrator response as a function of injection interval was studied. As the injection interval increased, the amount of sample trapped in the microconcentrator increased. However, once the interval equals t_b, the sample began to break through and the response could not be increased further. This is shown in Figure 4.8. So the response profile shows a linear increase in microtrap response up to t_b followed by a constant response beyond t_b.

Linearity in microconcentrator response was observed as a function of concentration. This was true even at different injection intervals. Since the amount of sample trapped in the microconcentrator was proportional to the concentration of the

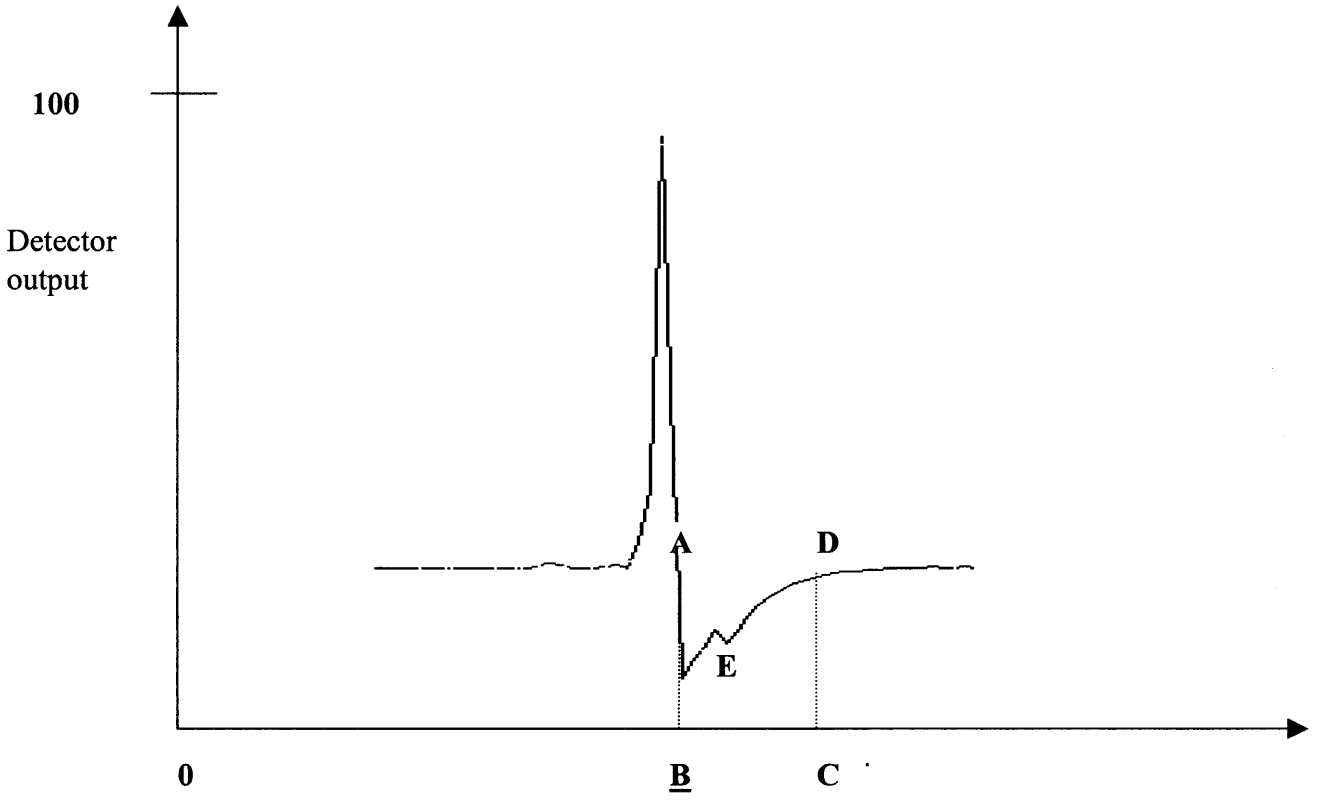

Figure 4.7 Characteristic peak from a low capacity microtrap which shows a pronounced negative peak.

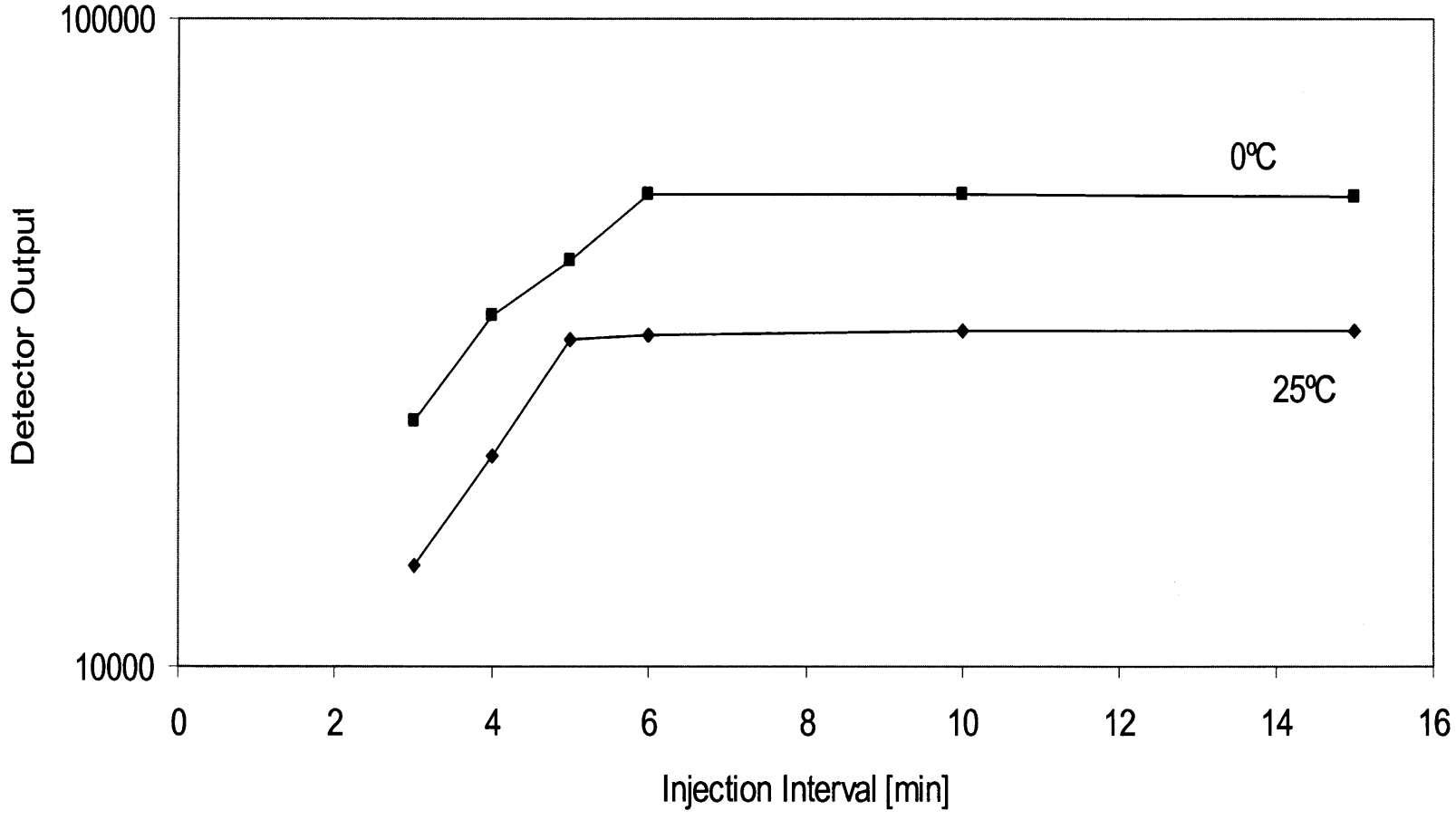

Figure 4.8 Microconcentrator response as a function of injection interval at 0 °C and 25°C. Toluene was used as the analyte.

stream flowing in, its response was proportional to sample concentration. At higher injection interval, the larger amount of trapped sample resulted in a higher response. The microconcentrator could be operated at any injection interval, either longer or shorter than t_b. Once beyond t_b, the sensitivity of the calibration curve did not increase. Operating it at higher frequency resulted in faster monitoring, but allowed less time for sample accumulation, thus, lower sensitivity.

4.3.3 Trapping Efficiency

Due to the small dimension of microconcentrator and limited amount of sorbent, it trapped only a fraction of the sample flowing through it and had relatively low capacity factor. However, the microconcentrator should accumulate as much sample as possible before making injection so that a large signal can be obtained at the sensor. The untrapped sample breaks through the microconcentrator. Trapping efficiency of the microconcentrator is defined as the fraction of the incoming sample retained by the microconcentrator before an injection is made:

$$\text{Trapping efficiency (T)} = \frac{\text{sample retained}}{\text{sample entering microconcentrator}} \qquad (4.2)$$

The retention mechanism in a microconcentrator is very similar to that of a GC column. There is equilibrium between the concentration of the sample in the polymer phase and the flowing gas phase. So trapping efficiency,

$$T = (t_b M_s) / t_i M_t \qquad (4.3)$$

$$T = (t_b M_s) / [t_i (M_s + M_m)] \qquad (4.4)$$

where, M_s is the amount of sample trapped per unit time in the polymer phase, M_t is the sample amount per unit time flowing into the microconcentrator, M_m is the amount of sample per unit time that remains in flowing gas phase and t_i is the injection interval. Since the capacity factor, k, is defined as,

$$k = M_s / M_m \tag{4.5}$$

Equation 4.5 reduces to :

$$T = (t_b / t_i)\, k / (k + 1) \tag{4.6}$$

The trapping efficiency was calculated from Equation 4.6. Figure 4.9 shows the trapping efficiency as a function of injection interval, t_i at two different microconcentrator temperatures. If the injection interval is less than the break through time, $t_i < t_b$, then Equation 4.6 becomes:

$$T = k / (k + 1) \tag{4.7}$$

and trapping efficiency depends only on the capacity factor of the microconcentrator.

As shown in Figure 4.9, when the injection interval is less then break through time, the trapping efficiency, T, is constant corresponding to the flat portion of the curve. When then injection interval is greater than break through time, i.e., $t_b < t_i$, the trapping efficiency decreases as predicted from Equation 4.6. The microconcentrator temperature affects the microconcentrator response. The trapping efficiency decreases with increase in microconcentrator temperature as shown in Figure 4.9. It it is seen that at 25°C, t_b was five minutes while t_b increased to six minutes at 0°C. Thus, the trapping efficiency was affected by the microconcentrator temperature. This is because a lower temperature

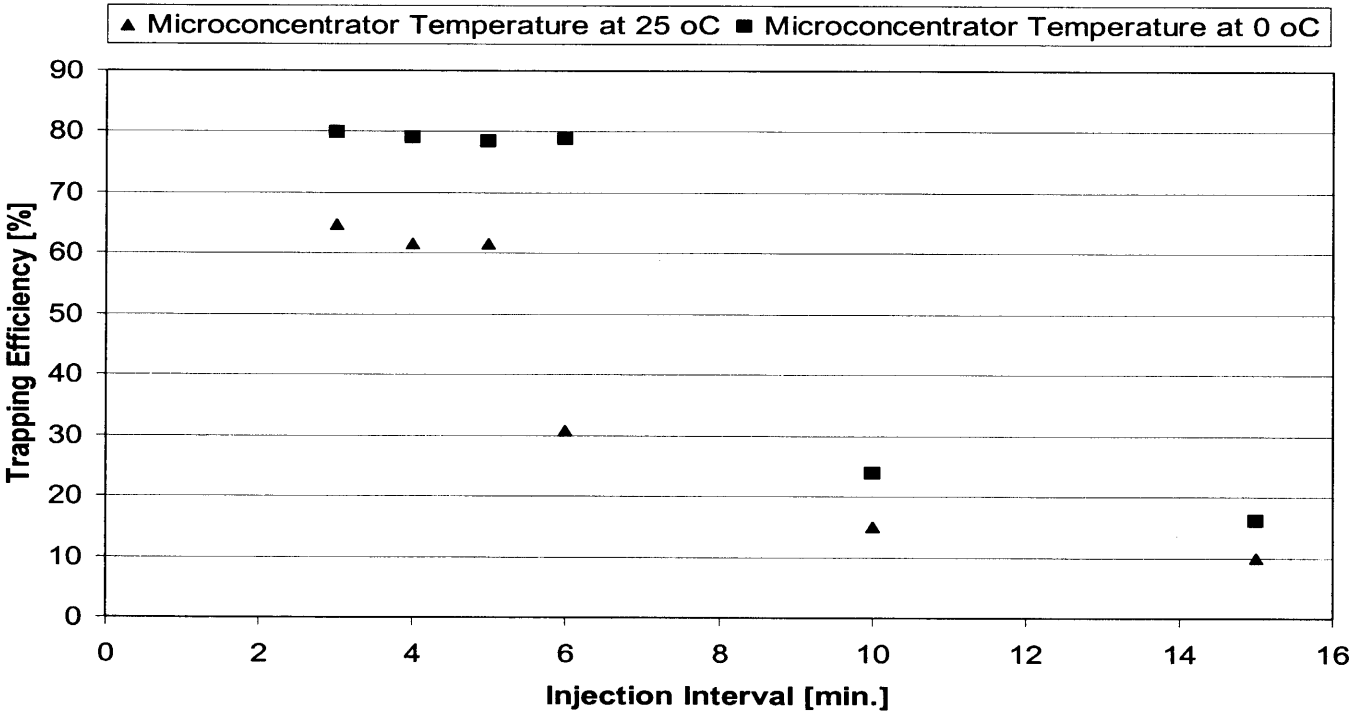

Figure 4.9 Trapping efficiency as a function of injection interval.

increases k in Equation 4.6, thus increasing trapping efficiency. High trapping efficiency generated a large signal and enhanced sensitivity.

4.3.4 Microconcentrator as a GC Injector

The microconcentrator was also used as a GC injector. A mixture of benzene, toluene and xylene were used as the sample stream. A short conventional GC column was used for the separation of these compounds. A series of injection were made and corresponding to each injection, a chromatogram was obtained. As shown in Figure 4.10, the sharp peaks and narrow bandwidths were observed. Reproducibility of retention time and peak high were very good for the microconcentrator. This can be used as an effective injector for gas chromatographs.

4.4 Microconcentrator Performance

The performance of the microconcentrator was studied in terms of linearity, precision, and detection limits. Calibration curves of toluene at 0 °C and 25 °C are presented in Figure 4.11. From the data, it was observed that a linear relationship between the response and toluene concentration existed in the interval concentration range of 20 – 800 ppm.

The microconcentrator precision was calculated by determining the relative standard deviation or RSD:

$$\text{RSD\%} = \text{Std. Dev.} / \text{Mean Conc.} \times 100 \qquad (4.8)$$

As shown in the Table 4.1, although the lowest concentration exhibited relatively higher variation, about 13% for Toluene at the 20ppm level, RSD% was in acceptable range.

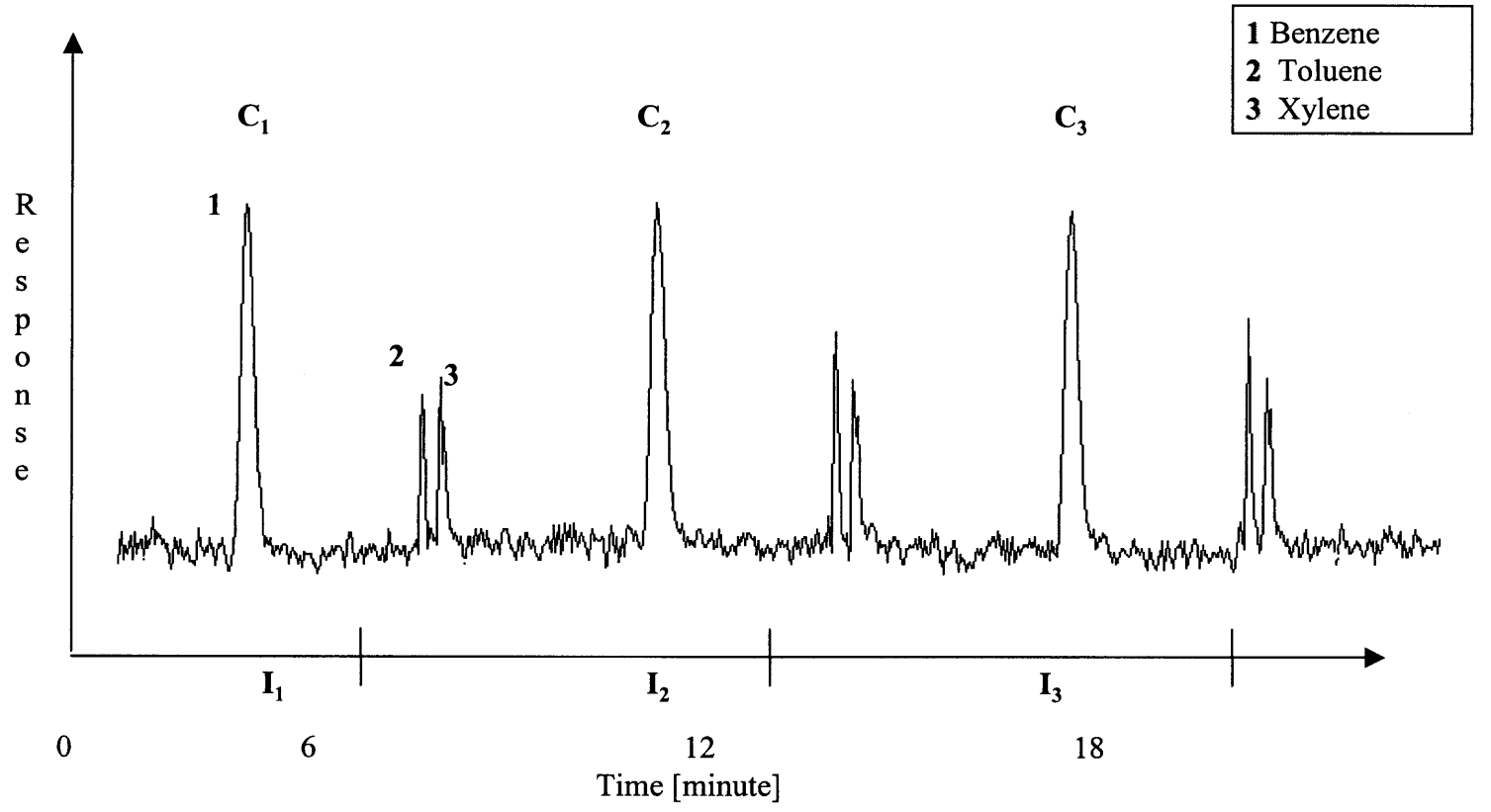

Figure 4.10 Continuous monitoring of a stream containing ppm levels of benzene, toluene and xylene. Corresponding to each injection I_1, I_2, I_3.... A response C_1, C_2, C_3....was obtained.

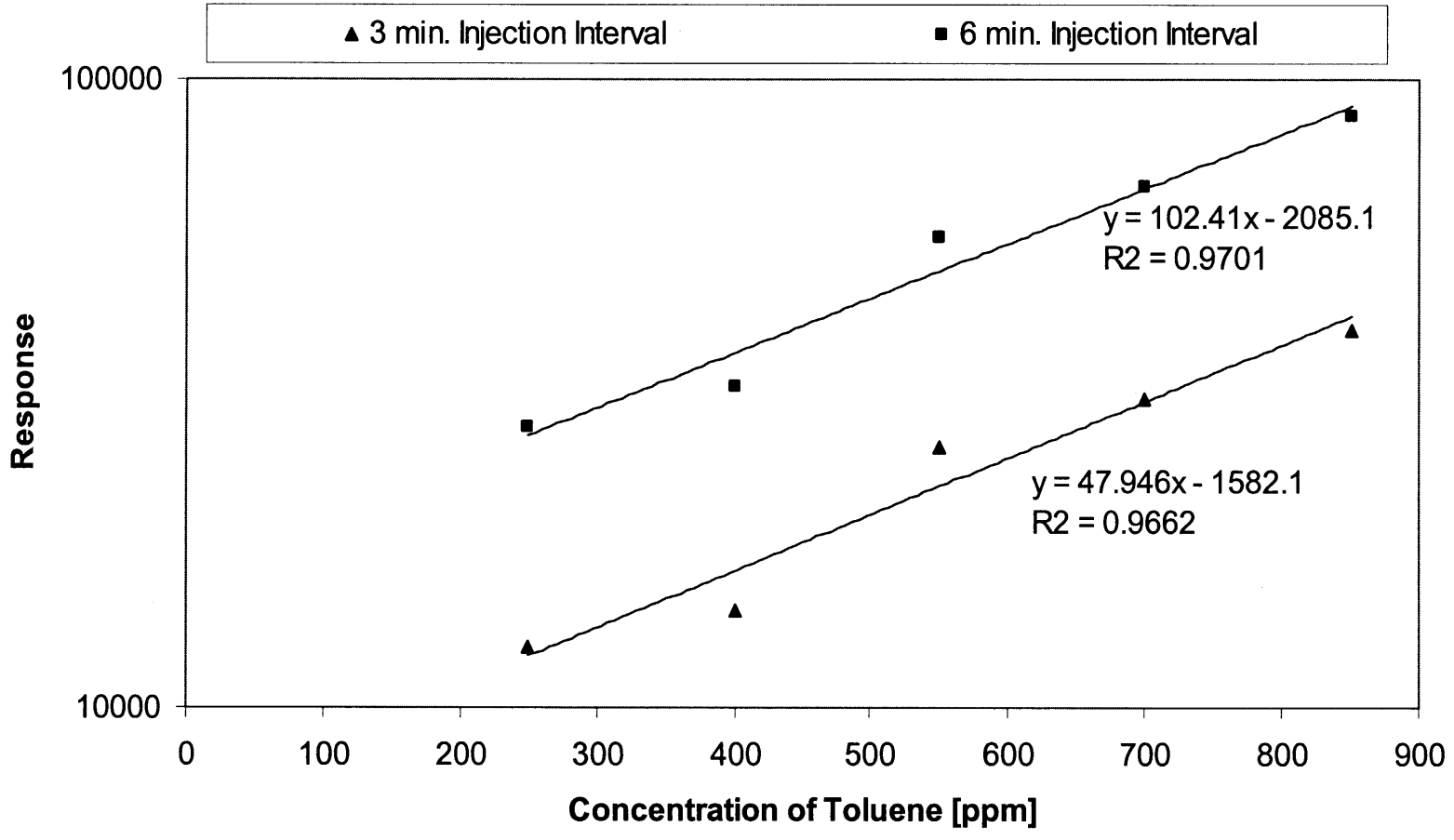

Figure 4.11 Microconcentrator response as a function of injection intervals, three and six minutes.

Table 4.1 Precision Analysis of Toluene using RSD%

Concentration of Toluene [ppm]	20	50	100	250	400	550	700	850
RSD%	13.32	3.42	5.32	2.73	3.02	5.34	3.55	2.38

Detection limit is roughly equal to 3 times the standard deviation of the blank over the slope of the calibration curve. However, the most generally accepted qualitative definition of detection limit is that it is the minimum concentration that can be measured with a known confidence level. Method detection limit (MDL) for Toluene was 8.4 ppm.

CHAPTER 5

CONCLUSION

Micromachined heaters using sputtered metal layer were fabricated during the first part of this research. Rapid heating to temperature as high as 360 °C was possible. It was also demonstrated that continual heating did not lead to devices weakening and burning out. Comparison with low dose boron implantation showed that the metal-deposited heaters were able to reach higher temperatures under the same conditions. Application of spin-on-glass on the heater surface, reduced the maximum attainable temperature, but still temperature as high as 100°C was possible. On the whole, it is concluded that deposition of metals to form a resistive layer is a simple and inexpensive method for fabricating heater for lab-on-a-chip applications.

During the second part of this research, the fabrication and characterization of a microfabricated microconcentrator was demonstrated. The preconcentration effect enhanced sensitivity and it was possible to use it as an injector for GC. The microconcentrator response was stable during long periods of operation and also producible.

APPENDIX A

THE TRAVELERS FOR THE DEVICE FABRICATION

Table A.1 shows the step by step processing to fabricate the microheater.

A.1 A Traveler for the Microheater

Stage	Process	Description	Date	Wafers	Operator	Comments
0. Start	Inspect	Starting material: P-type, 10-25Ω-cm, 6 inch, Single side polished.				
	Scribe	Scribe identification on the backside of the wafers				
	Scrub	High-pressure water				
1. Etch Mask (Deep)	Clean	M-pyrol: PRIMARY (95 °C) 10 min. SECONDARY (95 °C) 10 min. RINSE COLD DI 10 min. Spin dry				
	Clean	P – Clean: 5:1 H_2SO_4:H_2O_2 110°C 10 minutes Rinse Hot DI Water 10 min. Rinse Cold DI Water 5 min. Spin dry				

	Clean	RCA-2 clean: 4:1:1 H_2O:H_2O_2:HCl 80°C 10 min. Rinse Cold DI Water 5 min.				
	Pre-Clean	Furnace pre-clean: 100:1 H_2O: HF 1 minute Rinse Cold DI Water 10 min. Spin dry				
	Oxide	Stem Oxidation 2000 Å O_2: 7.5 SLM Bubbler: 530 sccm Temp: 1050°C Time: 20 min				
	Measure	Mean: Measured : 2015 Å #pts./wafer: 13 pts				
	Nitride	Deposit LPCVD Si_3N_4 DCS: 50 sccm Press: 300m Torr NH_3: 120 sccm Temp: 775°C Time: 23 min				
	Measure	Mean: Measured : 1565 Å #pts./wafer: 13 pts				
	Bake	Dehydration, oven 110°C, allow to cool				
	Prim	Prime Shipley 800 rpm 20 sec				

	Spin resist	Shipley 3813 2000 rpm 20 sec.				
	Bake	Hot plate #8 110 °C 1 min.				
	Expose	Front 15 sec Mask				
	Develop	Immersion develop First paddle 30 sec. Second paddle 60 sec.				
	Rinse, dry	Spin rinse, spin dry				
	Inspect	For residual resist and defects				
	Bake	Hard bake Hot plate #9 115 °C 60 sec.				
	Plasma Etch	Reactive Ion Etch Nitride/Oxide Trion-Phantom 40 sccm CF_4 250mTorr 150 watts 25 °C Time = ~ 2:20 each cycle				
	Inspect	Verify etching				

	Strip PR	M-pyrol: PRIMARY (95 °C) 10 min. SECONDARY (95 °C) 10 min. RINSE COLD DI 10 min. Spin dry				
	Etch	KOH etch silicon: 45% KOH 90 °C Etch rate 1.66Å /min Target 350 μm				
	Inspect	Inspect Etched to completion				
	Clean	RCA-2 clean: 4:1:1 H_2O:H_2O_2:HCl 80°C 10 min. Rinse Cold DI Water 5 min.				
	Clean	Furnace pre-clean: 100:1 H_2O: HF 1 minute Rinse Cold DI Water 10 min. Oven dry				
	Sputter	Target source: Al alloys Target thickness 1 μm				
	Prim	Prime Shipley 800 rpm 20 sec				

	Spin resist	Shipley 3813 2000 rpm 20 sec.				
	Bake	Hot plate #8 110 °C 1 min.				
	Expose	Front 15 sec Mask				
	Develop	Immersion develop First paddle 30 sec. Second paddle 60 sec.				
	Rinse, dry	Spin rinse, spin dry				
	Inspect	For residual resist and defects				
	Bake	Hard bake Hot plate #9 115 °C 60 sec.				
	Etch	Trion Etch Al-Cu-Si				
	Strip PR	M-pyrol: PRIMARY (95 °C) 10 min. SECONDARY (95 °C) 10 min. RINSE COLD DI 10 min. Spin dry				
	Spin SOG	Shipley 3813 2000 rpm 2 sec. SOG: 4 ml				

	Bake	Oven bake for 80 °C 150 °C 250 °C 40 sec. Each hot plate				
	Cure	Furnace curing 425 °C 60 min.				
	Inspect	Verify drying				

Table A.2 shows the step by step processing to fabricate the microconcentrator.

A.2 A Traveler for the Microconcentrator

Stage	Process	Description	Date	Wafers	Operator	Comments
0. Start	Inspect	Starting material: P-type, 10-25Ω-cm, 6 inch, Single side polished.				
	Scribe	Scribe identification on the backside of the wafers				
	Scrub	High-pressure water				
1. Etch Mask (Deep)	Clean	M-pyrol: PRIMARY (95 °C) 10 min. SECONDARY (95 °C) 10 min. RINSE COLD DI 10 min. Spin dry				
	Clean	P – Clean: 5:1 H_2SO_4:H_2O_2 110°C 10 minutes Rinse Hot DI Water 10 min. Rinse Cold DI Water 5 min. Spin dry				
	Clean	RCA-2 clean: 4:1:1 H_2O:H_2O_2:HCl 80°C 10 min. Rinse Cold DI Water 5 min.				

	Pre-Clean	Furnace pre-clean: 100:1 H_2O: HF 1 minute Rinse Cold DI Water 10 min. Spin dry				
	Oxide	Stem Oxidation 2000 Å O_2: 7.5 SLM Bubbler: 530 sccm Temp: 1050°C Time: 20 min				
	Measure	Mean: Measured : 2015 Å #pts./wafer: 13 pts				
	Nitride	Deposit LPCVD Si_3N_4 DCS: 50 sccm Press: 300m Torr NH_3: 120 sccm Temp: 775°C Time: 23 min				
	Measure	Mean: Measured : 1565 Å #pts./wafer: 13 pts				
	Bake	Dehydration, oven 110°C, allow to cool				
	Prim	Prime Shipley 800 rpm 20 sec				
	Spin resist	Shipley 3813 2000 rpm 20 sec.				
	Bake	Hot plate #8 110 °C 1 min.				

	Expose	Front 15 sec Mask				
	Develop	Immersion develop First paddle 30 sec. Second paddle 60 sec.				
	Rinse, dry	Spin rinse, spin dry				
	Inspect	For residual resist and defects				
	Bake	Hard bake Hot plate #9 115 °C 60 sec.				
	Plasma Etch	Reactive Ion Etch Nitride/Oxide Trion-Phantom 40 sccm CF_4 250mTorr 150 watts 25 °C Time = ~ 2:20 each cycle				
	Inspect	Verify etching				
	Strip PR	M-pyrol: PRIMARY (95 °C) 10 min. SECONDARY (95 °C) 10 min. RINSE COLD DI 10 min. Spin dry				

2. Silicon Etch	Etch	KOH etch silicon: 45% KOH 90 °C Etch rate 1.66Å /min Target 350 μm				
	Inspect	Inspect Etched to completion				
	Clean	RCA-2 clean: 4:1:1 H_2O:H_2O_2:HCl 80°C 10 min. Rinse Cold DI Water 5 min.				
3. Al Sputteri-ing	Clean	Furnace pre-clean: 100:1 H_2O: HF 1 minute Rinse Cold DI Water 10 min. Oven dry				
	Sputter	Target source: Al alloys Target thickness 1 μm				
	Prim	Prime Shipley 800 rpm 20 sec				
	Spin resist	Shipley 3813 2000 rpm 20 sec.				
	Bake	Hot plate #8 110 °C 1 min.				
	Expose	Front 15 sec Mask				

	Develop	Immersion develop First paddle 30 sec. Second paddle 60 sec.				
	Rinse, dry	Spin rinse, spin dry				
	Inspect	For residual resist and defects				
	Bake	Hard bake Hot plate #9 115 °C 60 sec.				
4. Al Etch	Etch	Trion Etch Al-Cu-Si				
	Strip PR	M-pyrol: PRIMARY (95 °C) 10 min. SECONDARY (95 °C) 10 min. RINSE COLD DI 10 min. Spin dry				
5. Spin-on-glass coating	Spin SOG	Shipley 3813 2000 rpm 2 sec. SOG: 4 ml				
	Bake	Oven bake for 80 °C 150 °C 250 °C 40 sec. Each hot plate				
	Cure	Furnace curing 425 °C 60 min.				
	Inspect	Verify drying				

6. Polymer Coating	*[1]Spin Polymer	Shipley 3813 800-2000 rpm				
	*[2]Bake	Oven bake for 48-72 hours				
		Repeat *[1] and *[2] steps				
	Inspect	Verify dring				

REFERENCES

1. J. Wang, "Portable electrochemical systems", *Trends in Anal. Chem.,* vol. 21, No. 4, pp. 226-232, 2002.

2. J. Wang, *Analytical Electrochemistry,* Wiley-VCH, NY, 2000.

3. W. Hancock, A. Apffel, J. Chakel, K. Hahnenberger, G. Choudhar, J. A. Traina and E. Pungor, *Anal. Chem.*, vol. 71, pp. 742A, 1999.

4. S. C. Jakeway, A. J. de Mello and E. Russell, "Miniaturized total analysis systems for biological analysis" *Fresentius J. Anal. Chem.,* vol. 366, No. 6/7, pp. 525, 2000.

5. T. Chovan and A. Guttman, "Microfabricated devices in biotechnology and biochemical processing, *Trends in Biotechnology,* vol. 20, No. 3, pp. 116-122, March 2002.

6. A. Manz, D. J. Harrison, E. Verpoorte, H. M. Widmer, in: P. R. Brown and E. Grushka (Editors), *Advan. in Chromatogr.,* Marcel Kekker, New York, pp. 1, 1993.

7. J. M. Ramsey, S. C. Jacobson and M. R. *Knapp, Nature Med.* Vol. 1, pp. 1093, 1995.

8. A. van den Berg, T. S. J. Lammerink, in: H. Becker and A. Manz (Editors), *Microsystem Technology in Chemistry and Life Science,* pp. 22, 1998.

9. J. P. Kutter, "Current developments in electroporetic and chromatographic separation methods on Microfabricated devices", *Trends in Anal. Chem.,* vol. 19, No. 6, pp. 352-363, 2000.

10. P-A. Auroux, D. Iossifidis, D. R. Reyes and A. Manz, "Micro Total Analysis Systems, 1. Introduction, Theory and Technology", *Anal. Chem.* vol. 74, No. 12, pp. 2623-2636, June 2002.

11. P-A. Auroux, D. Iossifidis, D. R. Reyes and A. Manz, "Micro Total Analysis Systems, 2. Analytical Standard Operations and Application", *Anal. Chem.* vol. 74, No. 12, pp. 2637-2652, June 2002.

12. A. Manz, D. J. Harrison, E. Verpoorte and H. M. Widmer, *Adv, Chromatogr,* vol. 33, pp. 1-66, 1993.

13. G. H. Sanders and A. Manz, *Trends Anal. Chem.,* vol. 19, pp. 364-378, 1993.

14. E. Verpoorte, *Electrophoresis*, vol. 23, pp. 677-712, 2002.

15. Sandia National Laboratories public web page on Sandia National Laboratories' Nonproliferation and Materials Control Program.

16. J. E. Parmeter, K.L. Linker, C. L. Rhykers, Jr., F. A. Bouchier and D. W. Hannum, "Development of a trace explosives detection portal for personnel screening", *Conference: IEEE 32nd Annual 1998 International Carnahan Conference on Security Technology,* October 12-14, VA, USA, 1998.

17. J. E. Parmeter, K.L. Linker, C. L. Rhykerd, Jr., F. A. Bouchier, D. W., Hannum, G. R. Eiceman and J. Rodriguez, "Personal portal for the trace detection of contraband material", *Conference: ONDCP Symposium*, 1999.

18. S. C. Terry and J. B. Angell, "A column gas chromatography system on a single wafer of silicon", Theory, Design, and Biomedical Applications of Solid State Chemical Sensors, P. W. Cheung, D. G. Fleming, M. R. Neuman, and W. H. Ko, Eds. Boca Raton, Fl: *CRC*, pp. 207-218, 1978.

19. 2. S. C. Terry, J. H. Jerman and J. B. Angell, "A gas chromatographic air analyzer fabricated on a silicon wafer", *IEEE Trans. Electron Devices*, vol. ED-26, pp. 1880-1886, December 1979.

20. 3. J. H. Jerman and S. C. Terry, "A miniature gas chromatograph for atmospheric monitoring", *Environ. Int.,* vol. 5, pp. 77-83, February 1981.

21. S. Saadat and S. C. Terry, "A high-speed chromatographic gas analyzer", *Amer. Lab.,* vol. 5, pp. 90-101, July 1984.

22. 5. A. van Es, J. Janssen, R. Bally, C. Cramers and J. Rijks, "Sample introduction in high speed capillary gas chromatography-Input band width and detection limits", J. High Res. *Chromatogr. Commun.,* vol. 10, pp. 273-279, May 1987.

23. 6. G. Lee, C. Ray, R. Siemers and R. Moore, "Recent developments in high speed gas chromatography", *Amer. Lab.,* vol. 21, pp. 108-119, February 1989.

24. 7. R. Siemers, D. Heigel and A. Spilkin, "Rapid micro-GC analysis of permanent gases", *Amer. Lab.,* vol. 23, pp. 44L-44R, March 1991.

25. S. Santy, A. Spilkin, and J. Strauss, "Rapid analysis of chlorofluorocarbons using a micro gas chromatograph", *Amer. Lab.,* vol. 23, p. 34, October 1991.

26. E. S. Kolesar, Jr. and R. R. Reston, "Review and summary of a silicon micromachined gas chromatography system", *IEEE Tran. on Comp., Pack. And Manufa. Tech.,* B, vol. 21, No. 4, pp. 324-328, November 1998.

27. E. S. Kolesar, Jr. and R. R. Reston, "Silicon micromachined gas chromatography system", Proc. Of the Annual IEEE Inter. Conf. On Innovative Systems in Silicon, October 8-10, TX, USA, pp. 117-125, 1997.

28. E. S. Kolesar, Jr. and R. R. Reston, "Design and fabrication of the fundamental components integrated to realize a functional silicon micromachined gas chromatography system", *American Society of Mechanical Engineers, Dynamic Systems and Control Division (Publication) DSC*, vol. 60, 1996, *Engineering Systems, Proceedings of the 1996 ASME International Mechanical Engineering Congress and Exposition*, November 17-22, Atlanta, GA, USA, pp. 11-17, 1996.

29. E. S. Kolesar, Jr. and R. R. Reston, "Miniature gas chromatography system realized using conventional VLSI fabrication techniques applied to quantifying toxic environmental pllutants", *IEEE Proc. of the National Aerospace and Electronics Conference,* vol. 1, pp. 327-333, 1994.

30. 9. R. R. Reston and E. S. Kolesar, "Silicon-micromachined gas chromatography system used to separate and detect ammonia and nitrogen dioxide-Part I: Design, fabrication and integration of the gas chromatography system", *IEEE/ASME J. Microelectromech. Syst.,* vol. 3, pp. 134-146, December 1994.

31. 10. E. S. Kolesar and R. R. Reston, "Silicon-micromachined gas chromatography system used to separate and detect ammonia and nitrogen dioxide-Part II: Evaluation, analysis and theoretical modeling of the gas chromatography system", *IEEE/ASME J. Microelectromech. Syst.,* vol. 3, pp. 147-154, December 1994.

32. A. Segal, T. Górecki, P. Mussche, J. Lips and J. Pawliszyn, "Development of membrane extraction with a sorbent interface-micro gas chromatography system for field analysis", *Journal of Chromatography. A*, vol. 873, No. 1, March 17, pp. 13-27, 2000.

33. C. M. Matzke, et al., "Microfabricated silicon gas chromatographic micro-channels: fabrication and performance", *Proceedings of the SPIE-the International Society for Optical Engineering*, vol. 3511, pp. 262-268, 1998.

34. Y. Kawamura, et al., "Analysis of hydrogen isotopes with a micro gas chromatograph", *Fusion Eng. Des.,* vol. 49-50, pp. 855-861, 2000.

35. Y. Kawamura, et al., "Development of a micro gas chromatograph for analysis of hydrogen isotope gas mixtures in the fusion fuel cycle", *Fusion Engineering and Design,* vol. 58-59, pp. 389-394, 2001.

36. A. J. de Mello, "Chip-MS: Coupling the large with the small", *Lab on a Chip,* vol. 1, pp. 7N-12N, 2001.

37. A. Shevchenko, I. Chernushevich, M. Wilm, M and M. Mann, "De Novo peptide sequencing by nanoelectrospray tandem mass spectrometry using triple quadrupole and quadrupole/time-of-flight instruments", *Methods in Molecular Biology (Clifton, N.J.),* volume 146, pp. 1-16, 2000.

38. E. J. Heller, V. M. Hietala, R. J. Kottenstette, R. P. Manginell, C. M. Matzke, P. R. Lewis, S. A. Casalnuovo, G. C. Frye-Mason, "An integrated surface acoustic wave based chemical microsensor array for gas-phase chemical analysis Microsystems", *Conference: Chemical Sensors IV,* 17-22 October, HI, USA, 1999.

39. M. Fang, K. Vetelino, M. Rothery, J. Hines and G. C. Frye, "Detection of organic chemicals by SAW sensor array", *Sensors and Actuators, B,* vol. 56, No. 1-2, pp. 155-157, July 1999.

40. G.C. Frye, S.J. Martin, R.W. Cernosek and K.B. Pfeifer. *Int. J. Environmentally Conscous*, vol. 1, p. 37, 1992.

41. J.W. Grate, S.L. Rose-Pehrsson, D.L. Venezky, *Anal. Chem.*, vol. 65, 1993.

42. M. Rapp, J. Reible, S. Stier, A. Voigt, J. Bahlo, *IEEE International Frequency Control Symposium,* Orlando, 1997.

43. M. Rapp, J. Reibel, A. Voigt, M. Balzer and O. Bulow, "New miniaturized SAW-sensor array for organic gas detection driven by multiplexed oscillators", *Sensors and Actuators, B*, vol. 65, No. 1-3, pp. 169-172, June 2000.

44. M. Rapp, B. Bob, A. Voigt, H. Gemmeke and H. J. Ache, "Develoment of an analytical microsystem for organic gas detection based on SAW resonators, *Fresenius' J. Anal. Chem.,* vol. 352, pp. 699-704, 1995.

45. M. Rapp, J. Reibel, S. Stier, A. Voigt and J. Bahlo, "SAGAS: gas analyzing sensor systems based on SAW devices- an issue of commercialization of SAW sensor technology", *Proc. of the IEEE Frequency Control Symp.,* pp. 129-132, 1997.

46. Mauder, "SAW gas sensors: comparison between delay line and two port resonator", *Sensor and Actuators, B,* vol. 26-27, pp. 187-190, 1995.

47. G. C. Frye-Mason, et al., "Microfabricated gas phase chemical analysis systems", *Conference: Microprocesses and Nanotechnology '99. 1999 International Microprocesses and Nanotechnology Conference*, 6-8 July, Japan, 1999.

48. E. T. Zellers, M. Morishits and Q-Y. Cai, "Evaluating porous-layr open-tubular capillaries as vapor preconcentrators in a microanalytical system", Sensors and Actuators, B, vol. 67, pp. 244-253, 2000.

49. S. C. Jakeway and A. J. de Mello, "Chip-based refractive index detection using a single point evanescent wave probe", *Analyst*, vol. 126, No. 9, pp. 1505-1510, 2001.

50. 50 G.J.M. Bruin, "Recent developments in electrokinetically driven analysis on microfabricated devices", *Electrophoresis,* pp. 3931-3951, 2000.

51. S.C. Terry, J.H. Jerman, and J.B. Angell, "A gas chromatographic air analyzer fabricated on a silicon wafer", *IEEE Trans, Electron Devl.,* vol. ED-26, pp. 1880-1886, 1979.

52. R.R. Reston and E.S. Kolesar, "Silicon-Micromachined Gas Chromatography System Used to Separate and Detect Ammonia and Nitrogen Dioxide- Part I: Design, Fabrication, and Integration of the Gas Chromatography System", *J. of Microelectromechanical systems,* vol. 3, No. 4, pp. 134-146, 1994.

53. M.L. Hudson, R. Kottenstette, C.M. Matzke, G.C. Frye-Mason, K.A. Shollenberger, D.R. Adkins, and C.C. Wong, Design, "Testing, and Simulation of Microscale Gas Chromatography Columns", *Micro-Electro-Mechanical Systems, ASME,* vol. 66, pp. 207-214, 1998.

54. A. Manz, Y. Miyahara, J. Miura, Y. Watanabe, H. Miyaqi, and K. Sato, "Design of an open-tubular column liquid chromatograph using silicon chip technology", *Sensors and Actuators, B,* pp. 249-255, 1990.

55. D.J. Harrison, P.G. Glavina, and A. Manz, "Towards miniaturized electrophoresis and chemical analysis systems on silicon: an alternative to chemical sensors", *Sensors and Actuators, B*, pp. 107-116, 1993.

56. D.J. Harrison, A. Manz, Z. Fan, H. Ludi, and H.M. Widmer, "Capillary electrophoresis and sample injection systems integrated on a planar glass chip", *Anal. Chem.,* vol. 64, No. 17, p. 1926, 1992.

57. S.C. Jacobson, R. Hergenroder, L.B. Koutny, R.J. Warmack, and J.M. Ramsey, "Effects of injection schemes and column geometry on the performance of microchip electrophoresis devices", *Anal. Chem.,* vol. 66, No. 7, pp. 1107-1113, 1994.

58. M. Freemantle, Downsizing Chemistry, *C&EN*, pp. 27-37, 1999.

59. R.K. Lowry, "Analytical Chemistry and the Microchip", *Anal. Chem.,* vol. 58, No. 1, pp. 23-34, 1986.

60. E.T. Lagally, P.C. Simpson, and R.A. Mathies, "Monolithic integrated microfluidic DNA amplification and capillary electrophoresis analysis system", *Sensors and Actuators, B*, pp. 138-146, 2000.

61. A.T. Woolley, D. Hadley, P. Landre, A.J. deMello, R.A. Mathies, and M.A. Northrup, "Functional Integration of PCR Amplification and Capillary Electrophoresis in a Microfabricated DNA Analysis Device", Anal. Chem., vol. 68, No. 23, pp. 4081-4086, 1996.

62. D.A. Benson, D. Bowman, W. Filter, and R. Mitchell, "Design and Characterization of Microscale Heater Structures for Test Die and Sensor Applications", Intersociety Conference on Thermal Phenomena, pp. 66-73, 1998.

63. S.W. Janson, "Batch-fabricated resistors: initial results", in *Proceedings of the International Electric Propulsion Conference, IEPC-97-070,* Cleveland, OH, USA, 1997.

64. L. Lin, K.S. Udell, and A.P. Pisano, "Vapor bubble formation on a micro heater in confined and unconfined micro channels", *Amer. Soc. of Mechanical Engineers, 29th National Heat Transfer Conference,* GA, USA, August 1993.

65. B.W. Chui, H.J. Mamin, B.D. Terris, D. Rugar, K.E. Goodson, and T.W. Kenny, "Micromachined heaters with 1-μs thermal time constants for AFM thermomechanical data storage", in *Proc. 1997 International Conference on Solid-State Sensors and Actuators (Transducers '97),* Chicago, USA, pp. 1085-1088 June1997.

66. R.L. Bayt and K.S. Breuer, "Analysis and testing of a silicon intrinsic-point heater in a micropropulsion application", *Sensors and Actuators, A,* pp. 249-255, 2001.

67. S. Wolf and R.N. Tauber, *Silicon Processing for the VLSI Era: Process Technology,* 2nd Edition, vol.1, Lattice Press, NY, USA, 1986.

68. C.A. Straede and N.J. Mikkelsen, "Industrial implementation of ion implantation on tools and wear parts based on a strategic approach", *Surface and Coatings Technology,* vol. 103-104, No. 1, pp. 191-194, 1998.

69. M.A. Rosa, S. Dimitrijev, and H.B. Harrison, "Fabrication and Analysis of Silicon Microbridge Heaters Micromachined from (100) SOI wafers", *MICRO '97,* pp. 108-112, 1997.

70. M.A. Rosa, S. Dimitrijev, H.B. Harrison, "KOH Wet Etching Techniques For The Micromachining OF (100) SOI Wafers", *COMMAD*, November 1996.

71. Z. Zhao, S. Glod, and D. Poulikakos, "Pressure and power generation during explosive vaporization on a thin-film microheater", *Inter. J. of Heat and Mass Transfer*, pp. 281-296, 2000.

72. S. Moller, J. Lin, and E. Obermeir, "Material and design considerations for low-power microheater modules for gas-sensing applications", *Sensors and Actuators, B,* pp. 343-346, 1995.

73. J. Gaspar, V. Chu, N. Louro, R. Cabeca, and J.P. Conde, "Thermal actuation of thin film microelectromechanical structures", *J. of Non-Crystalline Solids,* 2001, *uncorrected proof.*

74. S.C. Jacobson, A.W. Moore, and J.M. Ramsey, "Fused quartz substrates for microchip electrophoresis", *Anal. Chem.,* vol. 67, No. 13, pp. 2059-2063, 1995.

75. W. Kaplan, H. Elderstiq, and C. Vieider, "Novel fabrication method of capillary tubes on quartz for chemical analysis application", *Proceedings of the IEEE Micro Electro Mechanical Systems*, Piscataway, NJ, USA, pp. 63-68, 1994.

76. P.F. Man, D.K. Jones, and C.H. Mastranqelo, "Microfluidic plastic capillaries on silicon substrates: A new inexpensive technology for bioanalysis chips", *Proceedings of the IEEE Micro Electro Mechanical Systems,* Nagoya, Japan, January 1997.

77. P. Van Zant, *Microchip Fabrication*, 3rd Edition, McGraw-Hill, NY, USA, 1996.

78. M. Ohring, *The Materials Science of Thin Films*, Academic Press, CA, USA, 1992.

79. S.M. Sze, *Physics of Semiconductor Devices*, 2nd Edition, Wiley, John and Sons, Inc., NY, 1991.

80. K.G. Proctor, S.K. Ramirez, K.L. McWilliams, J.J. Kirkland, "In Chemically Modified Surfaces: Recent Developments", J.J. Pesek, M.T. Matyska, and R.R. Abuelafiya, *The Royal Society of Chemistry*, Cambridge, pp. 45-60, 1996.

81. J. J. Johnston, D. A. Goldade, D. J. Kohler and J. L. Cummings, *Environ. Sci. Technol.,* vol. 34, No. 9, pp. 1856-1861, 2000.

82. K. Dobosiewicz, K. Luks-Betlej and D. Bodzek, *Water, Air and Soil Pollution*, vol. 118, No. 1-2, pp. 101-113, 2000.

83. R. T. Short, D. P. Fries, G. P. G. Kibelka, S. K. Toler, P. G. Wenner and R. H. Byrne, *Oceans Conference Recored (IEEE),* vol. 1, Honolulu, HI, pp. 256-258, 2001.

84. J. A. De Gouw, C. J. Howard, T. G. Custer, B. M. Baker and R. Fall, *Environ. Sci. Technol.,* vol. 34, No. 12, pp. 2640-2648, 2000.

85. L. Charles, L. S. Riter and R. G. Riter, "Direct analysis of semivolatile organic compounds in air by atmospheric pressure chemical ionization mass spectrometry", *Anal. Chem.,* vol. 73, No. 21, pp. 5061-5065, 2001.

86. B. Galle, J. Samuelsson, B. H. Svensson and G. Borjesson, "Measurements of methane emissions from landfills using a time correlation tracer method based on FTIR absorption spectroscopy", *Environ. Sci. Technol.,* vol. 35, No. 1, pp. 21-25, 2001.

87. X. Hu, J. Nicholas, J. J. Zhang, M. Temi, P. De Filippis and P. K. Pradeep, "The destruction of N_2O in a pulsed corona discharge reactor", *Fue*l, vol. 81, No. 10, pp. 1259-1268, July 2002.

88. Y. Takao, Y. Kanda, Rev. *Sci. Instrum.,* vol. 67, No. 1, pp. 198-202, 1996.

89. S. Shelley, *Chem. Eng.,* pp. 30-37, 1991.

90. Q. H. Wu, K. M. Lee and C. C. Liu, "Development of chemical sensors using microfabrication and micromachining techniques", *Sensors and Actuators, B*, vol. 13, No. 1-3, pp. 1-6, May 1993.

91. B. van der Schoot, E. Verpoorte, S. Jeanneret, A. Manz and N. de Rooij, *Proceed. 1st Int. Symp. on Micro Total Analysis Systems, Twente, Netherlands,* pp. 21-22, 1994.

92. S. Zimmermann, S. Wischhusen and J. Mueller, "Micro flame ionization detector and micro flame spectrometer", *Sensors and Actuators, B,* vol. 63, No. 3, pp. 159-166, 2000.

93. H. Suzuki, Materials Science and Engineering C: *Biomimetic and Supramolecular Systems*, vol. 12, No. 1, pp. 55-61, 2000.

94. Th. Becker, St. Muehlberger, Chr. Bosch-v. Braunmuehl, G. Mueller, Th. Ziemann and K. V. Hechtenberg, *Sensors and Actuators, B,* vol. 69, No. 1, pp. 108-119, 2000.

95. C. Bulpitt and S. C. Tsang, "Detection and differentiation of C_4 hydrocarbon isomers over the Pd-SnO_2 compressed powder sensor, *Sensors and Actuators*, B, vol. 69, No. 1, pp. 100-107, 2000.

96. A. C. Romain, J. Nicolas, V. Wiertz, J. Maternova and Ph. Andre, "Use of a simple tin oxide sensor array to identify five malodours collected in the field, *Sensors and Actuators*, B, vol. 62, No. 1, pp. 73-79, 2000.

97. M. Fang, K. Vetelino, M. Rothery, J. Hines and G. C. Frye, "Detection of organic chemicals by SAW sensor array, *Sensors and Actuators,* B, vol. 56, No. 1-2, pp. 155-157, 1999.

98. J. Reibel, U. Stahla, T. Wessa and M. Rapp, "Gas analysis with SAW sensor systems", *Sensors and Actuators,* B, vol. 65, No. 1-3, pp. 173-175, 2000.

99. C. K. Kim, J. H. Lee, Y. H. Lee, N. I. Cho and D. J. Kim, "A study on a platinum-silicon carbide Schottky diode as a hydrogen gas sensor", *Sensors and Actuators, B,* vol. 66, No. 1, pp. 116-118, 2000.

100. J. Deng, W. Zhu, O. K. Tan and X. Yao, "Amorphous Pb(Zr, Ti)O_3 thin film hydrogen gas sensor, *Sensors and Actuators, B,* vol. 77, No. 1-2, pp. 416-420, 2001.

101. Y. Kawamura, S. Konishi and N. Masataka, *Fusion Eng. and Design*, vol. 58-59, pp. 389-394, 2001.

102. Agilent 3000 Micro GC, Agilent Technologies, U.S.A., 2002.

103. H. Noh, P. J. Hesketh and G. C. Frye-Mason, *Proceed. of the IEEE Micro Electro Mechanical Systems (MEMS)*, Las Vegas, NV, pp. 20-24, 2002.

104. W. Gopel, "Ultimate limits in the miniaturization of chemical sensors", *Sensors and Actuators, A,* vol. 56, No. 1-2, pp. 83-102, 1996.

105. M. J. Gardner, H. R. Rogers and S. D. W. Comber, *J. of Water Supply*, vol. 49, No. 2, pp. 103-109, 2000.

106. J. Beltran, F. J. Lopez, O. Cepria and F. Hernandez, "Solid-phase microextraction for quantitative analysis of organophosphorus pesticides in environmental water samples, *J. of Chromatogr, A,* vol. 808, No. 1-5, pp. 257-263, 1998.

107. Y. H. Xu and S. Mitra, "Continuous monitoring of volatile organic compounds in water using on-line membrane extraction and microtrap gas chromatography system, *J. of Chromatogr., A*, vol. 688, No. 1-2, pp. 171-180, 1994.

108. S. Mitra and C. Yun, "Continuous gas chromatographic monitoring of low concentration sample steams using an on-line microtrap", *J. of Chromatogr.*, vol. 648, No. 2, pp. 415-421, 1993.

109. S. Mitra, C. Feng, L. Zhang and W. Ho, Gary McAllister, *J. of Mass Spectrometry,* vol. 34, pp. 478-485, 1999.

110. S. Mitra, Y.H. Xu. W. Chen and G. McAllister, *J. of Air and Waste Management Assoc.,* vol. 48, pp. 643, 1998.

111. A. C. Savitsky and S. Siggia, *Anal. Chem.,* vol. 44, pp. 1712-1713, 1972.

112. M. Kim, S. Kishore, D. Misra and S. Mitra, submitted to *Sensors and Actuators*, 2002.

113. S. Mitra and J. B. Phillips, *J. Chromatogr. Sci.,* vol. 26, pp. 620-623, 1988.

114. M. Kim and S. Mitra, "A Microfabricated Microconcentrator for Sensors and Chromatographic Applications", submitted to *Anal. Chem.,* 2002.